

Abstract

HU, RUI. Error Analysis of the Immersed Interface Method for Elliptic Problems with an Interface. (Under the direction of Zhilin Li.)

The immersed interface method has been applied to a lot of interface problems. Error analysis of the immersed interface method for some interface problems with Dirichlet boundary conditions has shown that the immersed interface method gives second-order accurate numerical solutions. But the error analysis of the immersed interface method for problems with Neumann boundary conditions is still missing. During my PhD study, we have worked on error analysis of the immersed interface method for the Poisson interface problems with a Neumann boundary condition and the Stokes equations with an interface. For the Poisson interface equation with a constant coefficient, we use the method based on the results from Dr. Beale et al. With the discrete Poincare-Neumann inequality, we show that the numerical solution is second-order accurate. Next we consider the Poisson interface problem with a Neumann boundary condition and a piece-wise smooth coefficient. For this problem, an additional condition is needed to guarantee the problem well-posed. We use the method from the maximum principle and related theorems. A comparison function is constructed for the error estimation. From the result of the maximum principle and related theorems, it turns out that the immersed interface method is second-order accurate for the problems in both one-dimensional and two-dimensional spaces. After that, we consider a general elliptic problem with an interface and Neumann boundary conditions. But this problem is well-posed such that no additional condition is needed. We also use the method from the maximum principle and related theorems to show that the second-order accurate solution can be given by the immersed interface method. Finally we consider the static Stokes equations with an interface. We use the

three-Poisson-equations approach to decouple velocity and pressure in the Stokes equations. To preserve divergence-free of velocity, a Neumann boundary condition for pressure can be derived. Then our problem becomes three Poisson equations with an interface. We apply the result for the Poisson equation to show that the numerical solution of pressure is second-order accurate. With the result of analysis for pressure, we show that the numerical solutions of velocities are also second-order accurate.

© Copyright 2017 by Rui Hu

All Rights Reserved

Error Analysis of the Immersed Interface Method for Elliptic Problems with an
Interface

by
Rui Hu

A dissertation submitted to the Graduate Faculty of
North Carolina State University
in partial fulfillment of the
requirements for the Degree of
Doctor of Philosophy

Applied Mathematics

Raleigh, North Carolina

2017

APPROVED BY:

Stephen Schecter

Xiao-biao Lin

Negash Medhin

Zhilin Li
Chair of Advisory Committee

Dedication

To my family.

Biography

Rui Hu was born in Wuxi, China in the winter of 1988. After graduating with a B.S in applied mathematics from Shandong University, he decided to pursue further knowledge in mathematics. He got admitted in the Applied Mathematics graduated program in North Carolina State University in Raleigh, NC. He met Dr. Li and knew the research field about the finite difference method. Then he spent his time on doing researching about error analysis of the immersed interface method.

Acknowledgements

I would first like to thank Dr. Zhilin Li for guiding me during my PhD study. He is a person full of wisdom. The direction and support he provided while acting as a professional role model to me was invaluable and made my Ph.D study experience both insightful and worthwhile. I would also give thanks to my committee members Dr. Stephen Schecter, Dr. Xiao-biao Lin, Dr. Negash Medhin and Dr. Yichao Wu for their important support and feedback. Then I would like to give my thanks to my friends Daniel Godfrey and Steven Derochers for helping during my study. And I also would like to thank my parents. I could not advance so far without their support.

Table of Contents

LIST OF FIGURES	vii
Chapter 1 INTRODUCTION	1
1.1 Description of a one-dimensional problem	2
1.2 Description of a two-dimensional problem	4
1.3 Description of problems with irregular domain	5
1.4 The scope of the dissertation	6
1.5 Cartesian grid methods	7
1.6 Motivations of the dissertation	11
Chapter 2 ERROR ANALYSIS OF THE IMMERSED INTERFACE METHOD FOR THE POISSON EQUATIONS WITH AN INTERFACE	15
2.1 Review of jump conditions	16
2.2 Notations	18
2.3 Main convergence result	20
2.4 Proof of convergence	22
2.5 Conclusion	27
Chapter 3 ERROR ANALYSIS OF THE IMMERSED INTERFACE METHOD FOR THE POISSON EQUATIONS WITH AN INTERFACE AND VARIABLE COEFFICIENTS	29
3.1 The one-dimensional problem	30
3.1.1 A 1D two point boundary value problem with an interface and a Neumann boundary condition at one of endpoints	31
3.1.2 Reivew of the IIM for the 1D two point boundary value problem with an interface	32
3.1.3 Review of the maximum principle and related theorems	33
3.1.4 Main convergence result	36
3.1.5 A 1D two point boundary values problem with an interface and Neumann boundary conditions at both of endpoints	38
3.2 Analysis for the 2D problem	41
3.3 Conclusion	46
Chapter 4 ERROR ANALYSIS OF THE IMMERSED INTERFACE METHOD FOR A COMPLICATED ELLIPTIC PROBLEM	48
4.1 Review of the IIM	49
4.2 A comparison function	51
4.3 Main convergence result	54

4.4	Conclusion	56
Chapter 5 ERROR ANALYSIS OF THE IMMERSSED INTERFACE METHOD FOR THE INCOMPRESSIBLE STOKES EQUATIONS WITH AN INTERFACE		
5.1	Review of the three Poisson equations approach	57
5.1.1	Neumann boundary condition for the pressure	60
5.1.2	Proof of the equivalence and the divergence-free of velocity	62
5.2	Main convergence results	63
5.3	Proofs of theorem 5.2.1 and the lemma 5.2.2	65
5.4	The accuracy of velocity	68
5.4.1	The estimations of $D_1^+(p^h - p^e)$ and $D_2^+(p^h - p^e)$	73
5.4.2	The accuracy of velocity u and v	74
5.5	Conclusion	76
Chapter 6 CONCLUSION AND FUTURE WORK		
6.1	Summary	79
6.2	Future work	80
BIBLIOGRAPHY		82

LIST OF FIGURES

Figure 1.1	A diagram of a one-dimensional interface problem in domain $\Omega = [0, 1]$ with an immersed interface $x = \alpha$. $[u]$ and $[du/dx]$ are jump conditions at interface $x = \alpha$	2
Figure 1.2	A diagram of two materials in a domain Ω with an immersed interface Γ with subdomains Ω^- and Ω^+	4
Figure 1.3	A diagram of an irregular domain where the regions of Ω_2 are voids.	6
Figure 1.4	A diagram of a domain Ω with an immersed interface Γ . Cartesian grid is generated in Ω	8
Figure 2.1	A diagram of an interface Γ in the domain Ω , with the tangential $\boldsymbol{\tau}$ and normal direction \boldsymbol{n} at a point \mathbf{x}^* on the interface.	17
Figure 5.1	A diagram of an interface Γ in the domain Ω , with the tangential $\boldsymbol{\tau}$ and normal direction \boldsymbol{n} at a point \mathbf{x}^* on the interface.	58

Chapter 1

INTRODUCTION

In our daily life, there are many phenomena related to interface problems. When we have a singular force acting on a string, two different materials such as water and oil, or the same material at different states like water and ice, we are having an interface problem. For interface problems with fixed or moving interface, free boundary problems and problems in irregular domains, analytic solutions are rarely available. The immersed interface method is first introduced by LeVeque and Li in [17, 18, 19, 22], inspired by the immersed boundary method [23]. The immersed interface method can be applied on uniform or adaptive grids or triangulation in Cartesian/polar/spherical coordinates for many interface problems. Among the finite difference methods, it is one of the most efficient methods for solving one or higher dimensional problems. It modifies the numerical scheme near or on the interfaces to treat the irregularities and does not increase the computational cost significantly.

In the following sections, we show some examples of problems with a fixed interface to help us understand the immersed interface method.

1.1 Description of a one-dimensional problem

In this section, we start with a string with a singular force acting at a point, which is a one-dimensional interface problem. The system is shown in Figure 1.1. We can describe this system with the equations

$$u_{xx} = f(x), \quad 0 < x < 1, \quad (1.1)$$

$$u(0) = 0, \quad u(1) = 0, \quad (1.2)$$

where $u(x)$ is continuous, $f(x)$ is a source force

$$f(x) = v\delta_1(x - \alpha), \quad 0 < \alpha < 1. \quad (1.3)$$

Here δ_1 is a one-dimensional Dirac delta function and $x = \alpha$ is the point which we can treat as the interface.

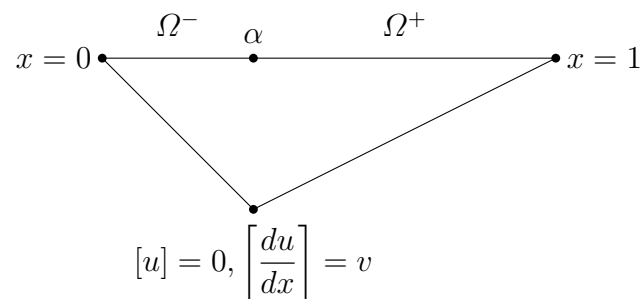


Figure 1.1 A diagram of a one-dimensional interface problem in domain $\Omega = [0, 1]$ with an immersed interface $x = \alpha$. $[u]$ and $[du/dx]$ are jump conditions at interface $x = \alpha$.

At $x = \alpha$, we have jump conditions

$$[u]|_{x=\alpha} = 0, \quad \left[\frac{du}{dx} \right] \Big|_{x=\alpha} = v, \quad (1.4)$$

which are defined as

$$[u](\alpha) = u^+(\alpha) - u^-(\alpha) \stackrel{\text{def}}{=} \lim_{x \rightarrow \alpha, x \in \Omega^+} u(x) - \lim_{x \rightarrow \alpha, x \in \Omega^-} u(x), \quad (1.5)$$

$$\left[\beta \frac{du}{dx} \right](\alpha) \stackrel{\text{def}}{=} \beta^+ \lim_{x \rightarrow \alpha, x \in \Omega^+} \frac{du}{dx}(x) - \beta^- \lim_{x \rightarrow \alpha, x \in \Omega^-} \frac{du}{dx}(x), \quad (1.6)$$

For this one-dimensional problem, we have the analytic solution:

$$u(x) = \begin{cases} -(1 - \alpha)x, & 0 \leq x < \alpha, \\ -\alpha(1 - x), & \alpha \leq x \leq 1. \end{cases} \quad (1.7)$$

To compute the numerical solution, we generate a Cartesian grid with step size h on the interval $[0, 1]$, with points $x_i = ih$. To compute numerical solution for our simple problem (1.1), (1.2), we can give a difference scheme at regular points x_i , $i \neq j, j + 1$ on the Cartesian grid

$$\frac{(U_{i+1} - U_i) - (U_i - U_{i-1}))}{h^2} = f_i, \quad (1.8)$$

where U_{i-1}, U_i, U_{i+1} are numerical solutions at x_{i-1}, x_i and x_{i+1} , with $f_i = f(x_i)$. Because of jump conditions at $x = \alpha$, the finite difference schemes at irregular grid points x_j and x_{j+1} , $x_j \leq \alpha \leq x_{j+1}$ are determined from the method of undetermined coefficients

$$\gamma_{j,1}U_{j-1} + \gamma_{j,2}U_j + \gamma_{j,3}U_{j+1} = f_j + C_j, \quad (1.9)$$

$$\gamma_{j+1,1}U_j + \gamma_{j+1,2}U_{j+1} + \gamma_{j+1,3}U_{j+2} = f_{j+1} + C_{j+1}, \quad (1.10)$$

where $\gamma_{j,1}$, $\gamma_{j,2}$, $\gamma_{j,3}$, $\gamma_{j+1,1}$, $\gamma_{j+1,2}$ and $\gamma_{j+1,3}$ are coefficients to be determined, and C_j and C_{j+1} are correction terms. We can minimize the truncation errors to determine these unknowns. The detail of regular and irregular grid points and truncation errors will be talked in Chapter 2.

1.2 Description of a two-dimensional problem

When we have two different materials which have different properties contacting along an interface such as water and oil, we have a two-dimensional interface problem. Such a system is shown in Figure 1.2.

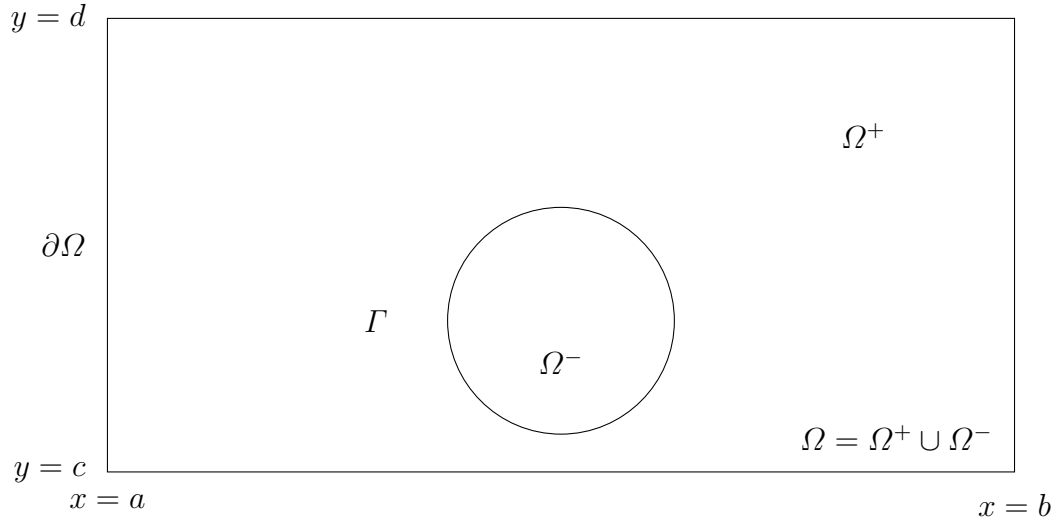


Figure 1.2 A diagram of two materials in a domain Ω with an immersed interface Γ with subdomains Ω^- and Ω^+ .

The mathematical description of the two-dimensional problem is

$$(\beta u_x)_x + (\beta u_y)_y = f(x, y), \quad a < x < b, \quad c < y < d, \quad (1.11)$$

$$u(a, y) = u_1, \quad u(b, y) = u_2, \quad u(x, c) = u_3, \quad u(x, d) = u_4, \quad (1.12)$$

where β is a constant or piece-wise smooth coefficient, and u is continuous while the flux of u is not. It implies that the jump conditions are

$$[u]_\Gamma = 0, \quad (1.13)$$

$$\left[\beta \frac{\partial u}{\partial \mathbf{n}} \right]_\Gamma = v, \quad (1.14)$$

which are defined as

$$[u](\mathbf{x}^*) = u^+(\mathbf{x}^*) - u^-(\mathbf{x}^*) \stackrel{\text{def}}{=} \lim_{\mathbf{x} \rightarrow \mathbf{x}^*, \mathbf{x} \in \Omega^+} u(\mathbf{x}) - \lim_{\mathbf{x} \rightarrow \mathbf{x}^*, \mathbf{x} \in \Omega^-} u(\mathbf{x}), \quad (1.15)$$

$$\left[\beta \frac{\partial u}{\partial \mathbf{n}}(\mathbf{x}^*) \right] \stackrel{\text{def}}{=} \beta^+ \lim_{\mathbf{x} \rightarrow \mathbf{x}^*, \mathbf{x} \in \Omega^+} \nabla u(\mathbf{x}) \cdot \mathbf{n}(\mathbf{x}) - \beta^- \lim_{\mathbf{x} \rightarrow \mathbf{x}^*, \mathbf{x} \in \Omega^-} \nabla u(\mathbf{x}) \cdot \mathbf{n}(\mathbf{x}), \quad (1.16)$$

where \mathbf{n} is the unit normal direction pointing to the Ω^+ side.

The different types of β make our problem different. In the later chapters of the dissertation, we talk about the problems with constant β and piece-wise constant β .

1.3 Description of problems with irregular domain

In our previous interface problems, we briefly discussed problems on a rectangular domain with still interface. While in the daily life, many interface problems occur on irregular domains. Figure 1.3 gives such an irregular domain.

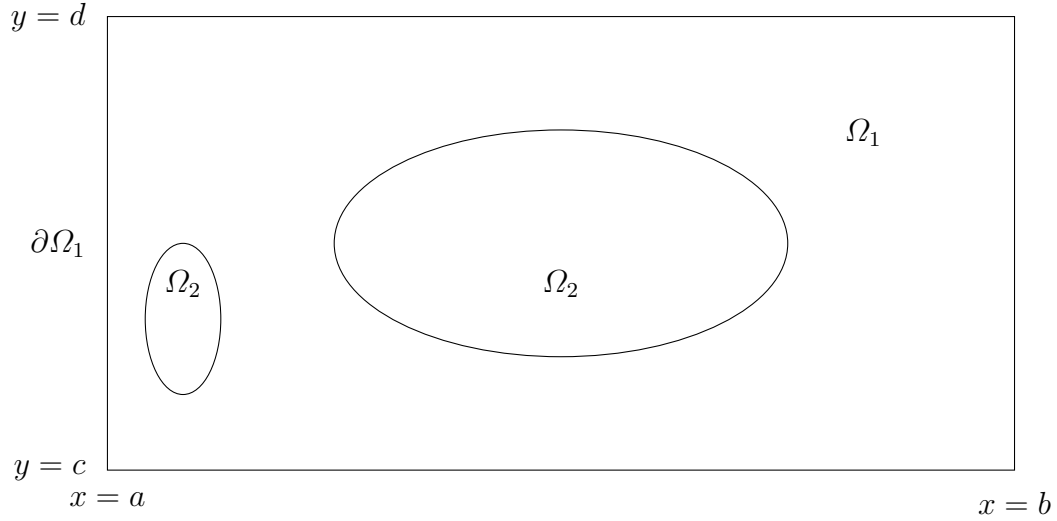


Figure 1.3 A diagram of an irregular domain where the regions of Ω_2 are voids.

The immersed interface method can be applied to a Poisson equation on such irregular domain in Section 6.2 from [22]. And an application of a fast Poisson solver on irregular domains, using the immersed interface method for an inversed problem of shape identification, is shown in Section 11.4 from [22].

1.4 The scope of the dissertation

We will focus on error analysis of elliptic interface problems with a Neumann boundary condition. We are going to concentrate our attention on problems with following features:

- The coefficients β in later problems may be constant or discontinuous across an interface.
- The source term at the right hand side of the moment equation may have jump or a delta function singularity along an interface.

- We assume that solutions to later problems are unique such that some additional conditions are needed.
- We only consider the problems with fixed interface and boundaries.
- The problems we consider have only one interface in the domain.

In the rest of the dissertation, we consider the immersed interface method in Cartesian grids.

1.5 Cartesian grid methods

To solve an interface problem using the immersed interface method, a computational grid or mesh must be provided. There are many ways to choose a grid such as a body fitted grid, or a mesh-less method. But in the following content of the dissertation, we will use fixed and uniform Cartesian grids. The Cartesian grid with step size h in two-dimensional domain $[a, b] \times [c, d]$ can be generated as in Figure 1.4.

One of the advantages of using a fixed and uniform Cartesian grid is that the generating process does not cost much. Numerical schemes can be used at most of the regular grid points. At irregular grid points, finite difference schemes can also be derived based on those standard finite difference schemes. Another advantage is that there are many software packages available on Cartesian grids such as the fast Poisson solver [29], the Clawpack [24] and the Amrclawpack [3], the level set method [11, 27, 28], the structured multigrid solver [1, 34] and many others.

For interface problems, besides the immersed interface method, there are many finite difference methods. In the following of this section, we discuss some important finite difference methods.

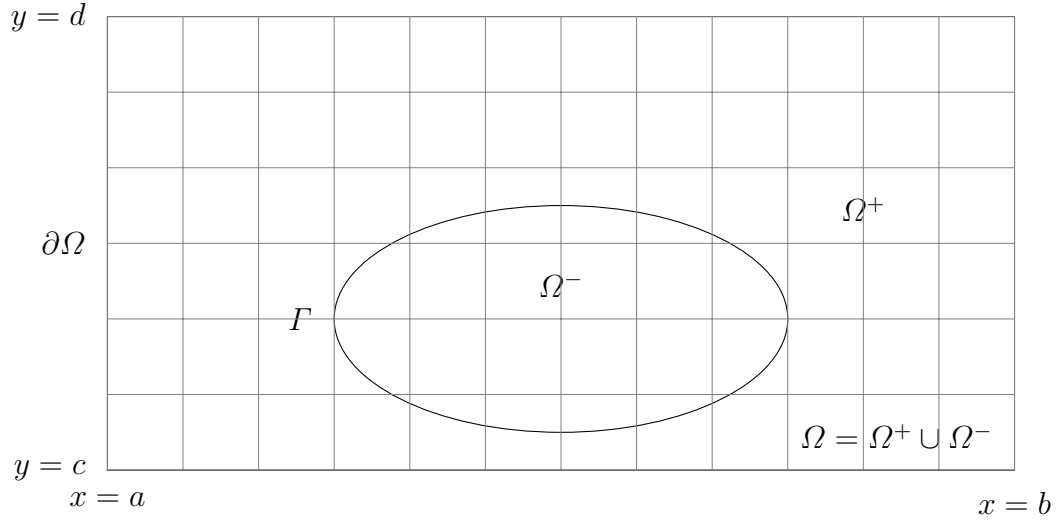


Figure 1.4 A diagram of a domain Ω with an immersed interface Γ . Cartesian grid is generated in Ω .

For one-dimensional problems, we assume we have a jump condition $[u] \neq 0$ for $u(x)$ at the interface $x = \alpha$. We can construct a smooth approximating function $u_\epsilon(x)$ by using the Heaviside function. This is called the smoothing method for discontinuous coefficients. The Heaviside function can be constructed in many ways. While it is easy to implement for one-dimensional problems, the numerical solution computed from the method may not be very accurate. And for two or higher dimensional problems, the Heaviside functions are not easy to be constructed and implemented.

Another method to deal with discontinuous coefficients in elliptic interface problems is harmonic averaging [12, 26, 30]. We consider a discrete scheme of a interface problem $(\beta u_x)_x = f$ on a Cartesian grid with step size h , where β is discontinuous

$$\frac{1}{h^2} \left(\beta_{i+\frac{1}{2}}(u_{i+1} - u_i) - \beta_{i-\frac{1}{2}}(u_i - u_{i-1}) \right) = f(x_i), \quad (1.17)$$

Because β is discontinuous in (x_{i-1}, x_{i+1}) , the harmonic average of β is

$$\beta_{i+\frac{1}{2}} = \left(\frac{1}{h} \int_{x_i}^{x_{i+1}} \beta^{-1}(x) dx \right)^{-1}. \quad (1.18)$$

This method is more accurate than the smoothing method for discontinuous coefficients. It can reach second order accuracy for one-dimensional elliptic interface problem with $[u]_{x=\alpha} = 0$, $[\beta u_x]_{x=\alpha} = 0$, and $[f]_{x=\alpha} = 0$, due primarily to the result of fortuitous cancellation. While the harmonic averaging is used for two-dimensional problems with discontinuous coefficients, we need to compute the harmonic average of $\beta(x, y)$ over squares [25]. In this way, the method may not give second order accuracy in general because the integration around the interface would be inaccurate.

Immersed boundary (IB) method was originally developed by Peskin [4, 5, 6, 7] to model blood flow in a human heart and has been applied to many other interface problems. One of important ideas in the immersed boundary (IB) method is using a discrete delta function to distribute a singular source to nearby grid points. For example, we can recall a discrete delta function

$$\delta_\epsilon(x) = \begin{cases} \frac{1}{4\epsilon}(1 + \cos(\pi x/2\epsilon)), & |x| < 2\epsilon, \\ 0, & |x| \geq 2\epsilon. \end{cases} \quad (1.19)$$

where ϵ is small enough. And it is easy to verify that the discrete delta function is continuous.

There are a lot of choices for the discrete delta function such as the hat function. With the discrete delta function, we can construct the discrete delta function for high dimensional problems, by taking the product of one dimensional discrete delta functions

such as $\delta_2(x, y) = \delta_1(x)\delta_1(y)$. Because of the continuity of the discrete delta function, we can discretize functions with jumps by using discrete delta function so that the singular source can be distributed to nearby grid points around interface. The details of the method can be found in [23]. Because the choice of discrete delta function can affect the accuracy of the numerical solution. Various studies have been conducted to find out what the best way to construct a Dirac delta function. For high-order problems, the immersed boundary method is easy to be implemented. But the work to improve the accuracy of the IB method is still being researched. Recent research [8, 31, 32] is focusing on the accuracy of the distribution.

Inspired by the immersed boundary (IB) method, the immersed interface method has been developed as a sharp interface method. In the immersed interface method introduced in [17], the discontinuity, or the jump conditions are enforced either exactly or approximately. For some problems, the immersed interface method is more efficient than a smoothing method. A numerical method called the immersed interface method, has the following features:

- A uniform or adaptive grid or triangulation in Cartesian, polar, or spherical coordinates is used instead of a body fitted grid. In this dissertation, we are using the uniform Cartesian grid with step size h .
- A prior knowledge of jump conditions (or internal boundary conditions) are known either from physical reasoning or from the governing differential equations. More interface relations often need to be derived from the given jump conditions and governing PDEs.
- Away from the interface, standard finite difference or finite element methods are used in the discretization. The numerical methods are modified according to the

jump conditions only at grid points or elements near or on the interface. In the dissertation, we focus on modifying the standard finite difference method by using jump conditions around the interface.

- We emphasize point-wise convergence. We are more concerned with errors in the infinity norm L^∞ . In regular problems without an interface, the immersed interface method generally has the same global order accuracy, often second order. However, the immersed interface method gives lower order accuracy for local truncation errors around the interface. Thus, the global infinity norm of errors is preferable.
- The finite difference method becomes the standard one if the discontinuities in the coefficients, in the solution, and in the flux, disappear.

1.6 Motivations of the dissertation

Solutions from numerical methods are approximating solutions to problems. Thus, error appears between numerical solutions and exact solutions. There is always error analysis along with numerical methods. In Section 1.4, when we discuss the finite difference methods, we have concerned about the accuracy of them. The smoothing method for discontinuous coefficients does not give very accurate solutions. The harmonic averaging does not guarantee a second order accurate solution, although it can give second order accurate solutions for specific interface problems. The accuracy of the immersed boundary (IB) method also depends on the discrete delta function we choose. For the immersed interface method, the local truncation errors of the finite difference scheme at regular points are $O(h^2)$. Meanwhile, the local truncation errors of the finite difference scheme at irregular points are $O(h)$. Whether the irregularity affects the global error

between numerical solution and exact solution becomes our question. In [2], Beale and Layton have shown the second order accuracy of immersed interface method for Poisson equation with an interface and a Dirichlet boundary condition. During the error analysis, they provide a lemma which split function at irregular points into the sum of terms of $O(h^2)$. We also can apply this lemma on our problem with a Neumann boundary condition. Moreover, in [9] the error analysis for the Poisson problems with discontinuities and Dirichlet boundary conditions, is given. Huang and Li give general results from Theorems (6.1) and (6.2) in [16]. If we want to use the results from Theorems (6.1) and (6.2), our problem needs to satisfy four conditions:

1. For each point in computational grid Ω_h , L_h has the form

$$L_h u^h(x_i) = \sum_k c_k u^h(x_k) - c_i u^h(x_i), \quad (1.20)$$

where the coefficients c_k and c_i are positive, L_h is the operator of finite difference scheme, u^h is numerical solution, and x_k are neighbor points of x_i . When x_i is near boundary, some values $u^h(x_k)$ at neighbor points are given by boundary conditions.

2. For each point in computational grid Ω_h ,

$$c_i \geq \sum_k c_k. \quad (1.21)$$

3. The domain Ω_h is connected. We say that a point x_i is connected to each of its neighbors that occurs in (1.20) with a non-zero coefficient. Then the domain is connected if any two points x_m and x_n in Ω_h , there is a sequence of points $x_m = x_{m_0}, x_{m_1}, \dots, x_{m_n} = x_n$ in Ω_h . And each x_{m_i} is connected to $x_{m_{i-1}}$ and $x_{m_{i+1}}$.

4. Dirichlet boundary conditions must be given on at least part of the boundary. This condition is needed to ensure uniqueness of solution.

With these conditions, in [9], Huang and Li use the maximum principle and related theorems to show that the immersed interface method for the Poisson equation with an interface and Dirichlet boundary conditions is second-order accurate. Using the similar method, Li and Ito in [22] have already shown that the immersed interface method reaches second order accuracy for two-dimensional and three-dimensional elliptic problems with Dirichlet boundary conditions. But the result for elliptic interface problems with Neumann boundary condition is still missing. For the problems with only Neumann boundary conditions, most of the solutions are not unique. This means that a solution can be shifted up and down to achieve different solutions which still satisfy our problem. Thus, our problem does not satisfy the uniqueness conditions mentioned above. To make our problem well-posed, additional conditions are needed.

To use the method from the discrete maximum principle, we need to construct a comparison function Φ . Sometimes it is not easy to construct the comparison function. Comparing with this method, the approach to show error analysis from [2] has an advantage that comparison function is not needed. But it does not work for problems with a variable coefficient $\beta(x)$.

Motivated by the method from [2] and another from the maximum principle and related theorems, we are going to show the error analysis of elliptic problems with an interface and a Neumann boundary condition. In the following dissertation, we will show that the immersed interface method reaches second-order accuracy for the Poisson interface problem with a Neumann boundary condition in Chapter 2, which is different from the problem with a Dirichlet boundary condition in [2]. In Chapter 3, we will use the

method from the maximum principle and related theorems to show the immersed interface method also reaches second-order accuracy for the Poisson interface problem with a piece-wise coefficient and a Neumann boundary condition. After it, we will discuss a more general elliptic problem with an interface and a Neumann boundary condition. For this Neumann boundary problem, no additional condition is needed to make the problem well-posed. The comparison function and result will be given in Chapter 4. Lastly, in [20], the author applies the immersed interface method to the Darcy-Stokes system with an interface. With refinement analysis, he shows that the numerical solution is second order accurate. The theoretical proof will be given later in this dissertation. We will consider the static Stokes equations with an interface and show that the numerical solution from the immersed interface method is second-order accurate in Chapter 5.

Chapter 2

ERROR ANALYSIS OF THE IMMERSED INTERFACE METHOD FOR THE POISSON EQUATIONS WITH AN INTERFACE

In this chapter, we consider the Poisson equation with constant coefficients in two-dimensional space,

$$\Delta u = f, \quad \mathbf{x} \in \Omega, \quad (2.1)$$

$$\left. \frac{\partial u}{\partial \mathbf{n}} \right|_{x \in \partial \Omega} = 0, \quad (2.2)$$

where u is the velocity, f is a continuous function in Ω . In [2], it has already shown that the immersed interface method reaches second-order accuracy for the Poisson equation with an interface and a Dirichlet boundary condition. But in this chapter, we are going to show that the immersed interface method also reaches second-order accuracy for the Poisson equation with an interface and a Neumann boundary condition.

2.1 Review of jump conditions

The interface $\Gamma \in C^2$ divides the domain into two disjoint sub-region Ω^+ and Ω^- . It is shown in Figure 2.1.

Because of the interface Γ , we have jump conditions on Γ ,

$$[u] = g_0 \quad \text{on} \quad \Gamma, \quad (2.3)$$

$$\left[\frac{\partial u}{\partial n} \right] = g_1 \quad \text{on} \quad \Gamma. \quad (2.4)$$

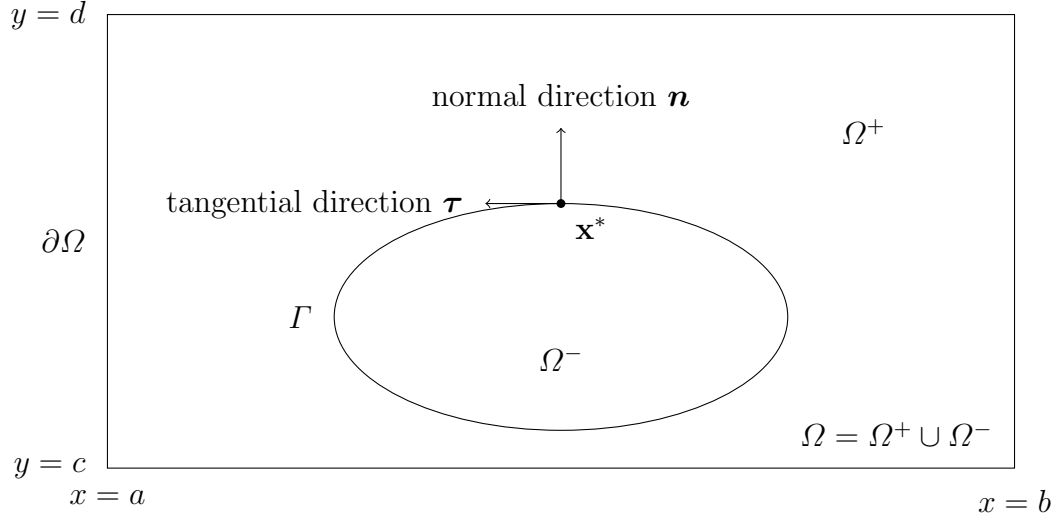


Figure 2.1 A diagram of an interface Γ in the domain Ω , with the tangential τ and normal direction \mathbf{n} at a point \mathbf{x}^* on the interface.

A jump quantity, for example, $[u]$ is defined as the difference of the limiting values from each side of the interface as follows,

$$[u](\mathbf{x}^*) = u^+(\mathbf{x}^*) - u^-(\mathbf{x}^*) \stackrel{\text{def}}{=} \lim_{\mathbf{x} \rightarrow \mathbf{x}^*, \mathbf{x} \in \Omega^+} u(\mathbf{x}) - \lim_{\mathbf{x} \rightarrow \mathbf{x}^*, \mathbf{x} \in \Omega^-} u(\mathbf{x}), \quad (2.5)$$

$$\left[\frac{\partial u}{\partial \mathbf{n}}(\mathbf{x}^*) \right] \stackrel{\text{def}}{=} \lim_{\mathbf{x} \rightarrow \mathbf{x}^*, \mathbf{x} \in \Omega^+} \nabla u(\mathbf{x}) \cdot \mathbf{n}(\mathbf{x}) - \lim_{\mathbf{x} \rightarrow \mathbf{x}^*, \mathbf{x} \in \Omega^-} \nabla u(\mathbf{x}) \cdot \mathbf{n}(\mathbf{x}), \quad (2.6)$$

where \mathbf{n} is the unit normal direction pointing to the Ω^+ side.

2.2 Notations

We follow the notations for discretization in [2]. The rectangular region Ω can be represented as

$$\Omega = \{x \in \mathbb{R}^2 : 0 < x < Nh, 0 < y < Mh\}. \quad (2.7)$$

Then, a grid can be generated on the region. We assume that we have a uniform grid with step size h . The computation domain is

$$\Omega_h = \{\mathbf{j}h = (j_1h, j_2h) \in h\mathbb{Z}^2 : 1 \leq j_1 \leq N - 1, 1 \leq j_2 \leq M - 1\}, \quad (2.8)$$

with boundary

$$\partial\Omega_h = \{\mathbf{j}h : 0 \leq j_1 \leq N, j_2 = 0 \text{ or } M; 0 \leq j_2 \leq M, j_1 = 0 \text{ or } N\}. \quad (2.9)$$

We use the usual second-order discrete Laplacian, defined for u^h on Ω_h as

$$\Delta_h u^h = D_1^- D_1^+ u^h + D_2^- D_2^+ u^h, \quad (2.10)$$

where D_k^\pm is the forward or backward difference operator in the x and y direction.

On the boundary, we define the first discrete finite difference stencil D_k^+ as

$$d_1 u(0, j_2 h) = \frac{u(h, j_2 h) - u(-h, j_2 h)}{2h}, \quad (2.11)$$

$$d_1 u(Nh, j_2 h) = \frac{u((N+1)h, j_2 h) - u((N-1)h, j_2 h)}{2h}, \quad (2.12)$$

$$d_2 u(j_1 h, 0) = \frac{u(j_1 h, h) - u(j_1 h, -h)}{2h}, \quad (2.13)$$

$$d_2 u(j_1 h, Mh) = \frac{u(j_1 h, (M+1)h) - u(j_1 h, (M-1)h)}{2h}. \quad (2.14)$$

We call a grid point **regular** if all grid points in the standard five-point stencil of the discrete Laplacian at the point are in the same region. Otherwise it is **irregular**. Let u^e be the exact solution. At regular grid points we have truncation error

$$\Delta_h u^e(\mathbf{j}h) = f_{\pm}(\mathbf{j}h) + \tau^h(\mathbf{j}h), \quad \|\tau^h(\mathbf{j}h)\| \leq Ch^2, \quad (2.15)$$

where f_{\pm} is based on whether $\mathbf{j}h \in \Omega_+$ or Ω_- . When we consider the error at irregular point, we have $T^h(\mathbf{j}h)$, determined by jumps on Γ

$$\Delta_h u^e(\mathbf{j}h) = f_{\pm}(\mathbf{j}h) + T^h(\mathbf{j}h) + \tau^h(\mathbf{j}h), \quad \|\tau^h(\mathbf{j}h)\| \leq Ch. \quad (2.16)$$

We define f^h on Ω_h by

$$f^h(\mathbf{j}h) = \begin{cases} f_{\pm}(\mathbf{j}h) + T^h(\mathbf{j}h), & \mathbf{j}h \text{ irregular,} \\ f_{\pm}(\mathbf{j}h), & \mathbf{j}h \text{ regular.} \end{cases} \quad (2.17)$$

Thus, we have u^h as the solution to the following problem

$$\Delta_h u^h = f^h \quad \text{in } \Omega_h, \quad du^h = O(h^2) \quad \text{on } \partial\Omega_h. \quad (2.18)$$

Then, the error $p^h - p^e$ satisfies

$$\Delta_h(u^h - u^e) = -\tau^h \quad \text{in } \Omega_h, \quad d(u^h - u^e) = -O(h^2) \quad \text{on } \partial\Omega_h. \quad (2.19)$$

2.3 Main convergence result

We can state our results with a Neumann boundary condition which is different from the result in [2]. After the theorem and related lemmas, proofs will be given. The theorem implies that the error in (2.19) is uniformly $O(h^2)$:

Theorem 2.3.1. *Let u^e be the exact solution of the Poisson equation (2.1), (2.2) with the interface Γ at least C^2 . Suppose $\Delta_h u^e$ has the form given by (2.15),(2.16), with $\|\tau_h(\mathbf{j}h)\| \leq Ch$ at irregular grid points and $\|\tau_h(\mathbf{j}h)\| \leq Ch^2$ at regular grid points. Let u^h be the solution to (2.17),(2.18). Assume that there is a chosen grid point (α, β) , where $u^h - u^e = 0$. Then,*

$$\|u^h - u^e\|_{\overline{\Omega}_h} = O(h^2). \quad (2.20)$$

Theorem 2.3.1 will follow directly from the next three lemmas. The first lemma is Lemma 2.2 in [2]:

Lemma 2.3.2. *Suppose F^{irr} is a function on Ω_h which is nonzero only on the set of irregular points. Assume Γ is C^1 . Then there exist functions F_1 and F_2 on $\overline{\Omega}_h$, so that $F_1 = F_2 = 0$ on $\partial\Omega_h$,*

$$F^{irr} = D_1^- F_1 + D_2^- F_2 \quad \text{in } \Omega_h, \quad (2.21)$$

and

$$\|F_k\|_{\overline{\Omega}_h} \leq Ch \|F^{irr}\|_{\overline{\Omega}_h}, \quad k = 1, 2, \quad (2.22)$$

where C depends on Γ but is independent of h .

Lemma 2.3.3. *Suppose*

$$\Delta_h v = F^{reg} + D_1^- F_1 + D_2^- F_2 \quad \text{in } \Omega_h, \quad dv = -O(h^2) \quad \text{on } \partial\Omega_h. \quad (2.23)$$

Then

$$\begin{aligned} \|\nabla_h^+ v\|_{\bar{\Omega}_h}^2 &\leq \|F^{reg}\|_{\bar{\Omega}_h} \|v\|_{\bar{\Omega}_h} + (\|F_1\|_{\bar{\Omega}_h} + O(h^4)) \|D_1^+ v\|_{\bar{\Omega}_h} \\ &\quad + (\|F_2\|_{\bar{\Omega}_h} + O(h^4)) \|D_2^+ v\|_{\bar{\Omega}_h} + 4O(h^3) \|v\|_{\bar{\Omega}_h}, \end{aligned} \quad (2.24)$$

where F^{reg} is a function on the set of regular points.

Next lemma is called Discrete Neumann-Poincare inequality:

Lemma 2.3.4. *If v is C^1 on Ω_h , we define*

$$A = v(c_1, c_2), \quad (2.25)$$

where (c_1, c_2) is a point on Ω_h .

Then,

$$\|v - A\|_{\bar{\Omega}_h} \leq C \|\nabla_h^+ v\|_{\bar{\Omega}_h}. \quad (2.26)$$

With these lemmas, to derive Theorem 2.3.1, we set F^{irr} equal to the restriction of τ^h at those irregular points and use Lemma 2.3.2. We apply Lemma 2.3.3 to $v = u^h - u^e$, using (2.19) with F^{reg} equal to the regular part of τ^h . To make the Poisson equation compatible, give a chosen point (α, β) where $v = 0$. We can set A in Lemma 2.3.4 as the error at point (α, β) . Combing (2.24) with Lemma 2.3.4, the result of the Theorem 2.3.1 can be derived.

In next section, we are going to show the proofs of lemmas and theorem.

2.4 Proof of convergence

Proof of Lemma 2.3.3. To show the inequality (2.24), we multiply by v in (2.23) over Ω_h . We have the usual discrete inner product,

$$(v, w)_{\overline{\Omega}_h} = \sum_{jh \in \overline{\Omega}_h} v(jh)w(jh)h^2. \quad (2.27)$$

With discrete inner product, we have

$$\|v\|_{\overline{\Omega}_h}^2 = (v, v)_{\overline{\Omega}_h}. \quad (2.28)$$

And then sum by parts on the left, using the Neumann boundary condition for v

$$\begin{aligned} (\Delta_h v, v)_{\overline{\Omega}_h} &= \sum_{jh \in \overline{\Omega}_h} (D_1^- D_1^+ v + D_2^- D_2^+ v) v h^2 \\ &= \sum_{jh \in \overline{\Omega}_h} D_1^- D_1^+ v \cdot v h^2 + \sum_{jh \in \overline{\Omega}_h} D_2^- D_2^+ v \cdot v h^2 \\ &= - \sum_{jh \in \overline{\Omega}_h} [(D_1^+ v)^2 + (D_2^+ v)^2] h^2 \\ &\quad + \sum_{j_2=0}^M [D_1^+ v(Nh, j_2h)]^2 \cdot h^2 + \sum_{j_1=0}^N [D_2^+ v(j_1h, Mh)]^2 \cdot h^2 \\ &\quad - \sum_{j_2=0}^M D_1^+ v(0, j_2h) \cdot v(0, j_2h) \cdot h \\ &\quad - \sum_{j_1=0}^N D_2^+ v(j_1h, 0) \cdot v(j_1h, 0) \cdot h \\ &\quad + \sum_{j_2=0}^M D_1^+ v(Nh, j_2h) \cdot v(Nh, j_2h) \cdot h \end{aligned} \quad (2.29)$$

$$+ \sum_{j_1=0}^N D_2^+ v(j_1 h, Mh) \cdot v(j_1 h, Mh) \cdot h.$$

From the discrete inner product

$$(\nabla_h^+ v, \nabla_h^+ v)_{\bar{\Omega}_h} = \sum_{jh \in \bar{\Omega}_h} [(D_1^+ v)^2 + (D_2^+ v)^2] h^2, \quad (2.30)$$

we have

$$\begin{aligned} (\Delta_h v, v)_{\bar{\Omega}_h} &= -(\nabla_h^+ v, \nabla_h^+ v)_{\bar{\Omega}_h} \\ &+ \sum_{j_2=0}^M [D_1^+ v(Nh, j_2 h)]^2 \cdot h^2 + \sum_{j_1=0}^N [D_2^+ v(j_1 h, Mh)]^2 \cdot h^2 \\ &- \sum_{j_2=0}^M D_1^+ v(0, j_2 h) \cdot v(0, j_2 h) \cdot h \\ &- \sum_{j_1=0}^N D_2^+ v(j_1 h, 0) \cdot v(j_1 h, 0) \cdot h \\ &+ \sum_{j_2=0}^M D_1^+ v(Nh, j_2 h) \cdot v(Nh, j_2 h) \cdot h \\ &+ \sum_{j_1=0}^N D_2^+ v(j_1 h, Mh) \cdot v(j_1 h, Mh) \cdot h. \end{aligned} \quad (2.31)$$

On the right hand side, we have

$$\begin{aligned} (F^{reg} + D_1^- F_1 + D_2^- F_2, v)_{\bar{\Omega}_h} &= (F^{reg}, v)_{\bar{\Omega}_h} \\ &+ (D_1^- F_1, v)_{\bar{\Omega}_h} + (D_2^- F_2, v)_{\bar{\Omega}_h}. \end{aligned} \quad (2.32)$$

Consider $(D_1^- F_1, v)$ and use summation by parts with $F_1 = 0$ on the boundary,

$$\begin{aligned}
(D_1^- F_1, v)_{\overline{\Omega}_h} &= \sum_{jh \in \overline{\Omega}_h} D_1^- F_1(j_1 h, j_2 h) v(j_1 h, j_2 h) h^2 \\
&= \sum_{jh \in \overline{\Omega}_h} [F_1(j_1 h, j_2 h) - F_1((j_1 - 1)h, j_2 h)] v(j_1 h, j_2 h) h \\
&= -(F_1, D_1^+ v) + \sum_{j_2=0}^M F_1(Nh, j_2 h) D_1^+ v(Nh, j_2 h) h^2 \\
&\quad - \sum_{j_2=0}^M F_1(0, j_2 h) v(0, j_2 h) h + \sum_{j_2=0}^M F_1(Nh, j_2 h) v(Nh, j_2 h) h \\
&= -(F_1, D_1^+ v)_{\overline{\Omega}_h}.
\end{aligned} \tag{2.33}$$

Similarly, we have

$$(D_2^- F_2, v)_{\overline{\Omega}_h} = -(F_2, D_2^+ v)_{\overline{\Omega}_h}. \tag{2.34}$$

Thus,

$$\begin{aligned}
(F^{reg} + D_1^- F_1 + D_2^- F_2, v)_{\overline{\Omega}_h} &= (F^{reg}, v)_{\overline{\Omega}_h} \\
&\quad - (F_1, D_1^+ v)_{\overline{\Omega}_h} - (F_2, D_2^+ v)_{\overline{\Omega}_h}.
\end{aligned} \tag{2.35}$$

Combining $(\Delta_h v, v)_{\overline{\Omega}_h}$ with $(F^{reg} + D_1^- F_1 + D_2^- F_2, v)_{\overline{\Omega}_h}$, we have

$$\begin{aligned}
(F^{reg}, v)_{\overline{\Omega}_h} - (F_1, D_1^+ v)_{\overline{\Omega}_h} - (F_2, D_2^+ v)_{\overline{\Omega}_h} &= -(\nabla_h^+ v, \nabla_h^+ v)_{\overline{\Omega}_h} \\
&\quad + \sum_{j_2=0}^M [D_1^+ v(Nh, j_2 h)]^2 \cdot h^2 + \sum_{j_1=0}^N [D_2^+ v(j_1 h, Mh)]^2 \cdot h^2 \\
&\quad - \sum_{j_2=0}^M D_1^+ v(0, j_2 h) \cdot v(0, j_2 h) \cdot h
\end{aligned} \tag{2.36}$$

$$\begin{aligned}
& - \sum_{j_1=0}^N D_2^+ v(j_1 h, 0) \cdot v(j_1 h, 0) \cdot h \\
& + \sum_{j_2=0}^M D_1^+ v(Nh, j_2 h) \cdot v(Nh, j_2 h) \cdot h \\
& + \sum_{j_1=0}^N D_2^+ v(j_1 h, Mh) \cdot v(j_1 h, Mh) \cdot h.
\end{aligned}$$

As we know, we defined D_1^+ and D_2^+ as central difference stencil on the boundary. We have

$$D_1^+ v = -O(h^2), D_2^+ v = -O(h^2) \quad \text{on the boundary.} \quad (2.37)$$

Thus, using Cauchy-Schwarz inequality we have inequality

$$\begin{aligned}
\|\nabla_h^+ v\|_{\overline{\Omega}_h}^2 & \leq \|F^{reg}\|_{\overline{\Omega}_h} \|v\|_{\overline{\Omega}_h} + (\|F_1\|_{\overline{\Omega}_h} + O(h^4)) \|D_1^+ v\|_{\overline{\Omega}_h} \\
& + (\|F_2\|_{\overline{\Omega}_h} + O(h^4)) \|D_2^+ v\|_{\overline{\Omega}_h} + 4O(h^3) \|v\|_{\overline{\Omega}_h}.
\end{aligned} \quad (2.38)$$

□

Proof of Lemma 2.3.4. For simplicity we consider the inequality in two dimensional space. We assume that there is a point $(c_1, c_2) \in \Omega$ such that

$$A = v(c_1, c_2). \quad (2.39)$$

For any grid point (x, y) on Ω_h

$$v(x, y) = v(c_1, c_2) + \sum_{\hat{x}=c_1}^x D_1^+ v(\hat{x}, c_2) h + \sum_{\hat{y}=c_2}^y D_2^+ v(c_1, \hat{y}) h \quad (2.40)$$

Taking the norm on Ω_h

$$\begin{aligned}
\|v - A\|_{\overline{\Omega}_h} &\leq \sum_{x=0}^{Nh} \|D_1^+ v(x, c_2)\|_{\overline{\Omega}_h} + \sum_{y=0}^{Mh} \|D_2^+ v(x, y)\|_{\overline{\Omega}_h} \\
&\leq (M + N) \|\nabla_h^+ v\|_{\overline{\Omega}_h} \\
&= C \|\nabla_h^+ v\|_{\overline{\Omega}_h}
\end{aligned} \tag{2.41}$$

□

Proof of Theorem 2.3.1. Let

$$v(x, y) = u^h(x, y) - u^e(x, y). \tag{2.42}$$

To make the Poisson equation (2.1),(2.2) with an interface compatible, we have $v(\alpha, \beta) = u^h(\alpha, \beta) - u^e(\alpha, \beta) = 0$. Then the Neumann-Poincare inequality becomes

$$\|v\|_{\overline{\Omega}_h} \leq C \|\nabla_h^+ v\|_{\overline{\Omega}_h}. \tag{2.43}$$

Back to the inequality (2.24) in Lemma 2.3.3, we have

$$\begin{aligned}
\|\nabla_h^+ v\|_{\overline{\Omega}_h}^2 &\leq \|F^{reg}\|_{\overline{\Omega}_h} \|v\|_{\overline{\Omega}_h} + (\|F_1\|_{\overline{\Omega}_h} + O(h^4)) \|D_1^+ v\|_{\overline{\Omega}_h} \\
&\quad + (\|F_2\|_{\overline{\Omega}_h} + O(h^4)) \|D_2^+ v\|_{\overline{\Omega}_h} + 4O(h^3) \|v\|_{\overline{\Omega}_h}.
\end{aligned} \tag{2.44}$$

With the discrete Neumann-Poincare inequality,

$$\begin{aligned}
\|\nabla_h^+ v\|_{\overline{\Omega}_h}^2 &\leq C \|F^{reg}\|_{\overline{\Omega}_h} \|\nabla_h^+ v\|_{\overline{\Omega}_h} + (\|F_1\|_{\overline{\Omega}_h} + O(h^4)) \|\nabla_h^+ v\|_{\overline{\Omega}_h} \\
&\quad + (\|F_2\|_{\overline{\Omega}_h} + O(h^4)) \|\nabla_h^+ v\|_{\overline{\Omega}_h} + 4CO(h^3) \|\nabla_h^+ v\|_{\overline{\Omega}_h}.
\end{aligned} \tag{2.45}$$

Divided by $\|\nabla_h^+ v\|_{\overline{\Omega}_h}$ on both sides

$$\begin{aligned} \|v\|_{\overline{\Omega}_h} &\leq C\|\nabla_h^+ v\|_{\overline{\Omega}_h} \leq C^2\|F^{reg}\|_{\overline{\Omega}_h} + C(\|F_1\|_{\overline{\Omega}_h} + O(h^4)) \\ &\quad + C(\|F_2\|_{\overline{\Omega}_h} + O(h^4)) + 4C^2O(h^3). \end{aligned} \tag{2.46}$$

According to the Lemma 2.3.2, we have

$$\|F_k\|_{\overline{\Omega}_h} = O(h^2), \quad \|F^{reg}\|_{\overline{\Omega}_h} = O(h^2), \tag{2.47}$$

$$\|v\|_{\overline{\Omega}_h} \leq (C^2 + 2C)O(h^2) + 2O(h^4) + 4C^2O(h^3). \tag{2.48}$$

This implies that

$$\|u^h(\mathbf{j}h) - u^e(\mathbf{j}h)\|_{\overline{\Omega}_h} = O(h^2) \quad \text{for } \mathbf{j}h \in \Omega_h. \tag{2.49}$$

□

Thus the proof of Theorem 2.3.1 is done.

2.5 Conclusion

In this chapter, we have error analysis of immersed interface method for the Poisson equation (2.1),(2.2) with an interface. Theorem 2.3.1 shows that the immersed interface method gives a second-order accurate numerical solution when the problem has a unique solution. Combining with the result from [2], we conclude that the immersed interface method gives a second-order accurate solution for the Poisson equation (2.1) with an interface, no matter whether the problem has a Dirichlet boundary condition or a Neumann

boundary condition.

Chapter 3

ERROR ANALYSIS OF THE IMMERSED INTERFACE METHOD FOR THE POISSON EQUATIONS WITH AN INTERFACE AND VARIABLE COEFFICIENTS

In this chapter, we discuss the Poisson equations with an interface, a variable coefficient and Neuman boundary conditions.

$$\nabla \cdot (\beta \nabla u) = f, \quad \mathbf{x} \in \Omega, \quad (3.1)$$

where u is velocity, $\beta(x)$ is a piece-wise smooth function which may have a finite jump at closed smooth interface $\Gamma \in \Omega$ and f is continuous. There are jump conditions along Γ :

$$[u] = g_0, \quad \left[\beta \frac{\partial u}{\partial n} \right] = g_1 \quad \text{on } \Gamma. \quad (3.2)$$

In [9, 22], they have already showed that the immersed interface method reaches second-order accuracy for the Poisson equation with an interface, a variable coefficient and Dirichlet boundary conditions. They use the method from the maximum principle and related theorems (6.1) and (6.2) in [16] to prove it. What if the boundary condition is a Neumann boundary condition? In this chapter, we extend the result from the maximum principle and related theorems to the interface problem with a Neumann boundary condition. Then we show that the immersed interface method gives a second-order accurate numerical solution for the interface problem with a Neumann boundary condition.

3.1 The one-dimensional problem

First of all, we start with a 1D two point boundary value problem with a Dirichlet boundary condition at an endpoint and a Neumann boundary condition at another endpoint.

3.1.1 A 1D two point boundary value problem with an interface and a Neumann boundary condition at one of endpoints

Consider a 1D two point boundary value problem with a Neumann boundary condition at one of the endpoints.

$$(\beta(x)u_x)_x = f(x), \quad 0 < x < 1, \quad (3.3)$$

$$\frac{\partial u}{\partial x}\Big|_{x=0} = u_1, \quad u|_{x=1} = u_2, \quad (3.4)$$

where $\beta(x)$ is a piece-wise smooth function. For simplicity, we assume

$$\beta(x) = \begin{cases} \beta^-, & \text{if } x \leq \alpha, \\ \beta^+, & \text{if } x > \alpha, \end{cases} \quad (3.5)$$

where $x = \alpha$ is the interface in the one-dimensional problem. At the interface $x = \alpha$, we have jump conditions as defined in Chapter 2

$$[u] = g_0, \quad \left[\beta \frac{\partial u}{\partial x} \right] = g_1. \quad (3.6)$$

It is easy to verify that the one-dimensional problem (3.3),(3.4) has a unique solution $u(x)$. Next, we review the finite difference scheme by using IIM from [22].

3.1.2 Reivew of the IIM for the 1D two point boundary value problem with an interface

According to the immersed interface method (IIM), we have a uniform grid $x_i = ih$, $i = 0, 1, \dots, n$ with step size $h = \frac{1}{n}$. Assuming that $x_j \leq \alpha \leq x_{j+1}$, we have general finite difference scheme

$$L_h u = \gamma_{i,1} u^h(x_{i-1}) + \gamma_{i,2} u^h(x_i) + \gamma_{i,3} u^h(x_{i+1}) = f(x_i), \quad (3.7)$$

with boundary conditions $\frac{\partial u}{\partial x} \Big|_{x=0} = u_1$ and $u|_{x=1} = u_2$.

As we have defined regular points and irregular points in Chapter 2, at a regular point x_i which means $i \neq j, j+1$, the coefficients $\gamma_{i,1}$, $\gamma_{i,2}$ and $\gamma_{i,3}$ are represented as

$$\gamma_{i,1} = \frac{\beta(x_{i-1/2})}{h^2}, \quad (3.8)$$

$$\gamma_{i,2} = -(\gamma_{i,1} + \gamma_{i,3}), \quad (3.9)$$

$$\gamma_{i,3} = \frac{\beta(x_{i+1/2})}{h^2}, \quad (3.10)$$

where $x_{i-1/2} = (x_i + x_{i-1})/2$ and $x_{i+1/2} = (x_i + x_{i+1})/2$. At the irregular grid point x_j , $\gamma_{i,1}$, $\gamma_{i,2}$ and $\gamma_{i,3}$ should satisfy the following linear system

$$\gamma_{i,1} + \gamma_{i,2} + \gamma_{i,3} = 0, \quad (3.11)$$

$$(x_{j-1} - \alpha)\gamma_{i,1} + (x_j - \alpha)\gamma_{i,2} + \frac{\beta^-}{\beta^+}(x_{j+1} - \alpha)\gamma_{i,3} = 0, \quad (3.12)$$

$$\frac{1}{2}(\alpha - x_{j-1})^2\gamma_{i,1} + \frac{1}{2}(\alpha - x_j)^2\gamma_{i,2} + \frac{\beta^-}{2\beta^+}(x_{j+1} - \alpha)^2\gamma_{i,3} = \beta^-. \quad (3.13)$$

This linear system is derived in [22]. After solving the linear systems at irregular

points x_j and x_{j+1} , we have the coefficients:

$$\begin{cases} \gamma_{j,1} = (\beta^- - [\beta](x_j - \alpha)/h)/D_j, \\ \gamma_{j,2} = (-2\beta^- + [\beta](x_{j-1} - \alpha)/h)/D_j, \\ \gamma_{j,3} = \beta^+/D_j, \end{cases} \quad (3.14)$$

$$\begin{cases} \gamma_{j+1,1} = \beta^-/D_{j+1}, \\ \gamma_{j+1,2} = (-2\beta^+ + [\beta](x_{j+2} - \alpha)/h)/D_{j+1}, \\ \gamma_{j+1,3} = (\beta^+ - [\beta](x_{j+1} - \alpha)/h)/D_{j+1}, \end{cases} \quad (3.15)$$

where

$$D_j = h^2 + [\beta](x_{j-1} - \alpha)(x_j - \alpha)/2\beta^-, \quad (3.16)$$

$$D_{j+1} = h^2 - [\beta](x_{j+2} - \alpha)(x_{j+1} - \alpha)/2\beta^+. \quad (3.17)$$

Now we have the finite difference scheme. We are going to use the method from the maximum principle and related theorems to show that the numerical solution are second-order accurate. In next subsection, we review the method from the maximum principle and related theorems.

3.1.3 Review of the maximum principle and related theorems

Before we recall the maximum principle, we need to recall four conditions which are introduced in [16]:

1. For each point $x_i \in \Omega_h$, L_h has the form:

$$L_h u^h(x_i) = \sum_k c_k u^h(x_k) - c_i u^h(x_i), \quad (3.18)$$

where the coefficients in 3.18 are positive. And x_k are neighbor points of x_i . When x_i is near boundary, some of values $u^h(x_k)$ at neighbor points can be given by boundary conditions.

2. For each point $x_i \in \Omega_h$,

$$c_i \geq \sum_k c_k. \quad (3.19)$$

3. The domain Ω_h is connected. We say that a point x_i is connected to each of its neighbors that occurs in 3.18 with a non-zero coefficient. Then the domain is connected if any two points x_m and x_n in Ω_h , there is a sequence of points $x_m = x_{m_0}, x_{m_1}, \dots, x_{m_n} = x_n$ in Ω_h . And each x_{m_i} is connected to $x_{m_{i-1}}$ and $x_{m_{i+1}}$.
4. Dirichlet boundary conditions must be given on at least part of the boundary. This condition is needed to ensure uniqueness of solution to the problem (3.3),(3.4).

With the assumptions for finite difference scheme, we can claim that our problem (3.3), (3.4) satisfies all above conditions. Next we recall the maximum principle:

Lemma 3.1.1. (*Maximum Principle*) *Suppose that L_h , Ω_h and $\partial\Omega_h$ satisfy all the above conditions and that a mesh function u^h satisfies*

$$L_h u^h(x_i) \geq 0, \quad x_i \in \Omega_h. \quad (3.20)$$

Then u^h cannot attain a nonnegative maximum at an interior point,

$$\max_{x_i \in \Omega_h} u^h(x_i) \leq \max\{\max_{A \in \partial\Omega_h} u^h(A), 0\}. \quad (3.21)$$

With the maximum principle, we have Theorem (6.1), (6.2) from [16].

Theorem 3.1.2. *Suppose a nonnegative mesh function Φ is defined on $\Omega_h \cup \partial\Omega_h$ such that*

$$L_h\Phi(x_i) \geq 1, \quad x_i \in \Omega_h, \quad (3.22)$$

and that all four conditions are satisfied. Then the error $e(x_i) = u^h(x_i) - u^e(x_i)$ is bounded by

$$|e(x_i)| \leq \left[\max_{A \in \partial\Omega_h} \Phi(A) \right] \left[\max_{x_i \in \Omega_h} |T(x_i)| \right], \quad (3.23)$$

where u^h is the numerical solution and u^e is the exact solution.

Theorem 3.1.3. *Suppose that, in the notation of Theorem 3.1.2, the set Ω_h is partitioned into two disjoint sets*

$$\Omega_h = \Omega_1 \cup \Omega_2, \quad \Omega_1 \cap \Omega_2 = \emptyset, \quad (3.24)$$

the nonnegative mesh function Φ is defined on $\Omega_h \cup \partial\Omega_h$ and satisfies

$$L_h\Phi(x_i) \geq C_1 > 0, \quad x_i \in \Omega_1, \quad (3.25)$$

$$L_h\Phi(x_i) \geq C_2 > 0, \quad x_i \in \Omega_2, \quad (3.26)$$

and the truncation error of the approximation $L_h u^e(x) = f(x)$ satisfies

$$|T(x_i)| \leq T_1, \quad x_i \in \Omega_1, \quad (3.27)$$

$$|T(x_i)| \leq T_2, \quad x_i \in \Omega_2. \quad (3.28)$$

Then the error in the approximation is bounded by

$$|e(x_i)| \leq \left[\max_{A \in \partial \Omega_h} \Phi(A) \right] \max \left\{ \frac{T_1}{C_1}, \frac{T_2}{C_2} \right\}. \quad (3.29)$$

The proofs of the maximum principle, theorem 3.1.2 and theorem 3.1.3 are provided in [16]. With the lemma and theorems, we show the result for our problem (3.3), (3.4).

3.1.4 Main convergence result

Because our problem satisfies all conditions we've mentioned in subsection 3.1.3. We can apply Theorem 4 in [9], which is the straightforward result from the maximum principle and related theorems to our problem :

Theorem 3.1.4. *Assume $\beta(x)$ is piece-wise constant as in (3.5), then the error of the approximate solution obtained from the IIM is bounded by*

$$\|u^e(x_i) - u^h(x_i)\|_{\overline{\Omega}_h} \leq \frac{5\gamma_{max}M\Phi_{max}}{3}h^2, \quad (3.30)$$

where

$$\gamma_{max} = \max_{1 \leq j \leq n-1} \max_{k=1,2,3} \{|\gamma_{j,k}h^2|\}, \quad (3.31)$$

$$\Phi_{max} = \max(\Phi(0), \Phi(1)), \quad (3.32)$$

$$M = \max(M_{xxx}, M_{xxxx}). \quad (3.33)$$

Here, M_{xxx} and M_{xxxx} are:

$$M_{xxx} = \max \left\{ \max_{x < \alpha} |u'''(x)|, \max_{x > \alpha} |u'''(x)| \right\}, \quad (3.34)$$

$$M_{xxxx} = \max \left\{ \max_{x < \alpha} |u''''(x)|, \max_{x > \alpha} |u''''(x)| \right\}. \quad (3.35)$$

And $\Phi(x)$ is constructed comparison function given by:

$$\Phi(x) = \begin{cases} \frac{(x - \alpha)^2}{2\beta^-} + \frac{E_1(1 - \alpha)(\alpha - x)}{\beta^-} + \frac{E_2(\alpha - x_j)(x_j - x)}{\gamma_{j,1}h^3}, & \text{if } x \leq \alpha, \\ \frac{(x - \alpha)^2}{2\beta^+} + \frac{E_1\alpha(x - \alpha)}{\beta^+} + \frac{E_2(x_{j+1} - \alpha)(x - x_{j+1})}{\gamma_{j+1,3}h^3}, & \text{if } x > \alpha, \end{cases} \quad (3.36)$$

where E_1 and E_2 are constants.

According to Theorem 3.1.4, it implies that the immersed interface method reaches second-order accuracy for our one-dimensional problem (3.3), (3.4). To prove this theorem, in [9], a lemma is provided:

Lemma 3.1.5. *Given a difference scheme L_h defined on a discrete set of interior points Ω_h , we assume the following conditions hold:*

1. Ω_h can be partitioned into a number of disjoint regions

$$\Omega_h = \Omega_1 \cup \Omega_2 \cup \Omega_3 \cup \dots \cup \Omega_s, \quad \Omega_i \cap \Omega_k = \emptyset, \quad \text{if } i \neq k. \quad (3.37)$$

2. The truncation error of the difference scheme at a grid point p satisfies

$$|T(x)| \leq T_i, \quad x \in \Omega_i, \quad i = 1, 2, \dots, s. \quad (3.38)$$

3. There exists a nonnegative mesh function Φ defined on $\bigcup_{i=1}^s \Omega_i$ satisfying

$$L_h \Phi(x) \geq C_i > 0, \quad x \in \Omega_i, \quad i = 1, 2, \dots, s. \quad (3.39)$$

Then the global error of the numerical solution from the difference scheme at mesh points is bounded by

$$\|E_h\|_{\bar{\Omega}_h} \leq \left(\max_{A \in \partial \Omega_h} \Phi(A) \right) \max_{1 \leq i \leq s} \left\{ \frac{T_i}{C_i} \right\}. \quad (3.40)$$

The proofs of Theorem 3.1.4 and Lemma 3.1.4 are given in [9]. They can be directly used on our problem, although we have a Neumann boundary condition at one of endpoints and a Dirichlet boundary condition at the other one.

However we often have interface problems with Neumann boundary conditions all along the boundary. In a 1D two point boundary values problem with an interface, we have Neumann boundary conditions at both endpoints $x = 0$ and $x = 1$. In next subsection, we talk about this problem.

3.1.5 A 1D two point boundary values problem with an interface and Neumann boundary conditions at both of endpoints

In last subsection, we have already shown that the immersed interface method gives second-order accurate numerical solution for the 1D two point boundary value problem with an interface, a piece-wise smooth coefficient $\beta(x)$ and a Neumann boundary condition at one of endpoints of the interval. In this subsection, we talk about result of a 1D two point boundary values problem with an interface, a piece-wise smooth coefficient and Neumann boundary conditions at both of endpoints of the interval. The problem is

$$(\beta(x)u_x)_x = f(x), \quad 0 < x < 1, \quad (3.41)$$

$$\frac{\partial u}{\partial x} \Big|_{x=0} = u_1, \quad \frac{\partial u}{\partial x} \Big|_{x=1} = u_2, \quad (3.42)$$

with jump conditions at $x = \alpha$

$$[u] = g_0, \quad \left[\beta \frac{\partial u}{\partial x} \right] = g_1. \quad (3.43)$$

As we know, this problem does not have a unique solution because we can shift a solution up and down vertically to have many solutions. To make this problem well-posed, an additional condition is needed. We assume that

$$u(x_0) = u_0. \quad (3.44)$$

Thus, the four conditions we mentioned in subsection 3.1.3 are satisfied. Recall the comparison function (3.36)

$$\Phi(x) = \begin{cases} \frac{(x - \alpha)^2}{2\beta^-} + \frac{E_1(1 - \alpha)(\alpha - x)}{\beta^-} + \frac{E_2(\alpha - x_j)(x_j - x)}{\gamma_{j,1}h^3}, & \text{if } x \leq \alpha, \\ \frac{(x - \alpha)^2}{2\beta^+} + \frac{E_1\alpha(x - \alpha)}{\beta^+} + \frac{E_2(x_{j+1} - \alpha)(x - x_{j+1})}{\gamma_{j+1,3}h^3}, & \text{if } x > \alpha, \end{cases} \quad (3.45)$$

On a Cartesian grid with step size h , we suppose that $x_j < \alpha < x_{j+1}$ which $x = \alpha$ is the interface. We have the finite difference scheme L_h defined by (3.7). We split $[0, 1]$

into

$$\Omega_0 = \{x_0, x_n\}, \quad (3.46)$$

$$\Omega_1 = \{x_1, x_2, \dots, x_{j-1}\}, \quad (3.47)$$

$$\Omega_2 = \{x_{j+2}, x_{j+3}, \dots, x_{n-1}\}, \quad (3.48)$$

$$\Omega_3 = \{x_j, x_{j+1}\}. \quad (3.49)$$

According to the results in [9], on $\Omega_1 \cup \Omega_2$,

$$L_h \Phi(x_i) = 1. \quad (3.50)$$

On Ω_3 ,

$$L_h \Phi(x_j) = 1 + \frac{E_1 \gamma_{j,3} (x_{j+1} - \alpha)}{\beta^+} + \frac{E_2 (\alpha - x_j)}{h^2} \geq \frac{1}{h}, \quad (3.51)$$

$$L_h \Phi(x_{j+1}) = 1 + \frac{E_1 \gamma_{j+1,1} (\alpha - x_j)}{\beta^-} + \frac{E_2 (x_{j+1} - \alpha)}{h^2} \geq \frac{1}{h} \quad (3.52)$$

On Ω_0 ,

$$\Phi(x_0) = \frac{\alpha^2}{2\beta^-} + \frac{E_1 (1 - \alpha) \alpha}{\beta^-} + \frac{E_2 (\alpha - x_j) x_j}{\gamma_{j,1} h^3} = O(1), \quad (3.53)$$

$$\Phi(x_n) = \frac{(1 - \alpha)^2}{2\beta^+} + \frac{E_1 \alpha (1 - \alpha)}{\beta^+} + \frac{E_2 (x_{j+1} - \alpha) (1 - x_{j+1})}{\gamma_{j+1,3} h^3} = O(1). \quad (3.54)$$

We know that the truncation error $|T_i| = O(h^2)$ in $\Omega_1 \cup \Omega_2$ and $|T_j| = O(h)$, $|T_{j+1}| = O(h)$ in Ω_3 . Using the result from Lemma 3.1.5, the global error of the numerical solution

from the immersed interface method is bounded by

$$\|u^h - u^e\|_{\bar{\Omega}_h} \leq \left(\max_{A \in \Omega_0} \Phi(A) \right) \max_{x_i} \left\{ \frac{T_i}{C_i} \right\} = O(h^2). \quad (3.55)$$

Thus, we have the result of the 1D two point boundary values problem with an interface, a piece-wise smooth coefficient $\beta(x)$ and Neumann boundary conditions at both of endpoints in the domain $[0, 1]$:

Theorem 3.1.6. *For the problem (3.41), (3.42), (3.43), we assume that $\beta(x)$ is piece-wise smooth. We have $u(x_0) = u_0$ such that the solution of the problem is unique. Then the error of the numerical solution obtained from the immersed interface method is second-order accurate*

$$\|u^h - u^e\|_{\bar{\Omega}_h} = O(h^2). \quad (3.56)$$

The proof can be shown following above analysis with the result from Lemma 3.1.5.

3.2 Analysis for the 2D problem

In the previous section, we show the results of one-dimensional problems with an interface and Neumann boundary conditions. For problems in two-dimensional space, does the immersed interface method still give the second-order accurate numerical solution as one-dimensional problems? In [22], Dr. Li et al have shown that the immersed interface method gives second order accurate numerical solutions for two-dimensional Poisson equations with an interface and Dirichlet boundary conditions. They also use the method from the maximum principle and related theorems. We talk about the interface problem with a Neumann boundary condition in this section. We consider the Poisson equation

with an interface

$$(\beta u_x)_x + (\beta u_y)_y = f(x, y), \quad (x, y) \in \Omega = \Omega^+ \cap \Omega^-, \quad (3.57)$$

with Neumann boundary condition

$$\frac{\partial u(x, y)}{\partial \mathbf{n}} = u_1 < \infty, \quad (x, y) \in \partial\Omega, \quad (3.58)$$

where \mathbf{n} is the normal vector along $\partial\Omega$. β is piece-wise continuous and has finite discontinuities across interface. $f(x, y)$ is continuous on Ω . Two jump conditions are defined around interface

$$[u] = u^+ - u^- = u_2, \quad (3.59)$$

$$\left[\beta \frac{\partial u}{\partial \mathbf{n}} \right] = \beta^+ \frac{\partial u^+}{\partial \mathbf{n}} - \beta^- \frac{\partial u^-}{\partial \mathbf{n}} = u_3. \quad (3.60)$$

To make this problem well-posed, an additional condition is needed:

$$u(a, b) = u_0 < \infty, \quad (a, b) \in \Omega. \quad (3.61)$$

Thus, a solution to the problem exists and is unique. We use a two-dimensional Cartesian grid with step size h on Ω . From the results in [22], the standard 9-point compact stencil is preferred because the resulting linear system of equations are block tridiagonal such that the multigrid solver can be used. The general finite difference stencil in two dimensional space can be given as follows

$$L_h U_{ij} = \sum_k^{n_s} \gamma_k U_{i+i_k, j+j_k}, \quad (3.62)$$

where U_{ij} are numerical solutions to $u(x, y)$ at (x_i, y_j) , n_s is the number of grid points involved in the finite difference stencil and i_k, j_k take values in the set $\{0, \pm 1, \pm 2, \dots\}$.

To guarantee the finite difference scheme satisfies the conditions mentioned in Section 3.1.3, restrictions on coefficients $\{\gamma_k\}$ are given by

$$\gamma_k \geq 0 \quad \text{if} \quad (i_k, j_k) \neq (0, 0), \quad (3.63)$$

$$\gamma_k < 0 \quad \text{if} \quad (i_k, j_k) = (0, 0). \quad (3.64)$$

And an optimization problem for the finite difference scheme at irregular points is given to determine the coefficients in [22]. Thus, the results of coefficients are given by

$$\left| \frac{\gamma_k}{\beta^-} \right| \leq \frac{C}{h^2}, \quad k = 1, \dots, 9. \quad (3.65)$$

And there exists at least one γ_k from each side of the interface such that

$$\frac{\gamma_r}{\beta^-} \geq \frac{C_1}{h^2}, \quad (3.66)$$

and

$$\sum_{\xi_k \geq 0} \gamma_k \xi_k \geq \frac{C_2}{h} \quad \text{if} \quad \max_{\xi \geq 0} \{\xi_k\} > C_3 h, \quad (3.67)$$

where ξ_k are from local coordinates of points (x_k, y_k) . These results are verified in [22]. Because we have $u(a, b) = u_0 < \infty$ and the Neumann boundary condition $\frac{\partial u(x, y)}{\partial \mathbf{n}} =$

$u_1 < \infty$. The Taylor expansion of $u(a, b)$ at (x, y) can be given as follows

$$u(a, b) = u(x, y) + (a - x)u_x(x, y) + (b - y)u_y(x, y) + \dots \quad (3.68)$$

We rewrite it into

$$u(x, y) = u(a, b) - (a - x)u_x(x, y) - (b - y)u_y(x, y) - \dots \quad (3.69)$$

With $u(a, b) = u_0 < \infty$, $u_1 < \infty$ and continuous $f(x, y)$ on Ω , we can estimate that

$$u(x, y) < \infty, \quad (x, y) \in \partial\Omega. \quad (3.70)$$

There is a constant K big enough so that $u(x, y) \leq K$ on the boundary $\partial\Omega$.

To show result of the problem (3.57)-(3.61), we consider a simplified problem

$$(\beta u_x)_x + (\beta u_y)_y = 1, \quad (3.71)$$

$$[u] = 0, \quad \left[\beta \frac{\partial u}{\partial \mathbf{n}} \right] = 1, \quad (3.72)$$

$$\frac{\partial u(x, y)}{\partial \mathbf{n}} = 0, \quad u(a, b) = 1. \quad (3.73)$$

To use the method from the maximum principle and related theorems, we need to construct a comparison function. Supposing that Φ is the unique and bounded solution to the problem, we can construct a comparison function

$$\bar{\Phi}(x, y) = \Phi(x, y) + \left| \min_{(x, y) \in \Omega} \Phi(x, y) \right|. \quad (3.74)$$

Then we apply the stencil (3.62) to $\bar{\Phi}(x, y)$ according to [22]. Combining the result of

coefficients (3.67), we have

$$L_h \bar{\Phi}(x_i, y_j) \geq \begin{cases} 1 + O(h^2), & (x_i, y_j) \text{ is a regular grid point,} \\ \sum_{\xi_k \geq 0} \gamma_k \xi_k \geq \frac{C_2}{h} + O(1), & (x_i, y_j) \text{ is an irregular grid point.} \end{cases} \quad (3.75)$$

We have already known that at regular points, the truncation error of the finite difference scheme satisfies

$$\|T_{ij}\| \leq C_3 h^2. \quad (3.76)$$

And at irregular points, the truncation error of the finite difference scheme satisfies

$$\|T_{ij}\| \leq C_4 h. \quad (3.77)$$

From the result of Lemma 3.1.5, at regular points, we have:

$$\frac{\|T_{ij}\|}{L_h \bar{\Phi}(x_i, y_j)} \leq K \frac{C_3 h^2}{1} = K C_3 h^2. \quad (3.78)$$

At irregular points, we have:

$$\frac{\|T_{ij}\|}{L_h \bar{\Phi}(x_i, y_j)} \leq K \frac{C_4 h}{C_2/h} = \frac{K C_4}{C_2} h^2, \quad (3.79)$$

where K is the bound of the value of $u(x, y)$ on $\partial\Omega$.

With results above, the global error of the immersed interface method for our problem is bounded by

$$\|u^h - u^e\| \leq C h^2, \quad (3.80)$$

where u^h is the numerical solution from the immersed interface method and u^e is the

exact solution to our problem.

Thus, we conclude our result for the Poisson equation with an interface and a Neumann boundary condition:

Theorem 3.2.1. *Let $u^e(x, y)$ be the exact solution to the Poisson equation (3.57), (3.58), (3.59), (3.60) and (3.61) where $\beta(x)$ is piecewise continuous, $u \in C^3(\Omega)$ and $f(x, y)$ is continuous. On a Cartesian grid with small enough step size h , we use the standard compact 9-point stencil (3.62) at irregular points such that the coefficients of the scheme satisfy:*

$$|\gamma_k| \leq \frac{C_1}{h^2} \quad \text{and} \quad \sum_{\xi_k \geq 0} \gamma_k \xi_k \geq \frac{C_2}{h}, \quad (3.81)$$

where ξ_k is from the local coordinates (ξ_k, η_k) . Assume we have numerical solution $u^h(x, y)$ from the finite difference scheme, the error is bound by:

$$\|u^h - u^e\| \leq Ch^2, \quad (3.82)$$

where C is a constant.

3.3 Conclusion

In this section, we have shown that the immersed interface method gives a second-order accurate numerical solution for the Poisson equation with an interface and a Neumann boundary condition. We use the method from the maximum principle and related theorems in [16]. No matter whether the problem is one-dimensional or two-dimensional, the method can be applied. This method can also be used on a more complicated elliptic problem:

$$(\beta(x)u_x)_x - \sigma^2 u = f, \quad (3.83)$$

with an interface and Neumann boundary conditions. We talk about it in next Chapter.

Chapter 4

ERROR ANALYSIS OF THE IMMERSED INTERFACE METHOD FOR A COMPLICATED ELLIPTIC PROBLEM

In this chapter, we estimate the error from the immersed interface method for the following elliptic problem

$$(\beta(x)u_x(x))_x - \sigma^2 u(x) = f(x), \quad x \in \Omega = (0, 1), \quad (4.1)$$

where $\beta(x)$ is positive piece-wise continuous. For simplicity, we have

$$\beta(x) = \begin{cases} \beta^-, & x < \alpha, \\ \beta^+, & x \geq \alpha. \end{cases} \quad (4.2)$$

And around the interface $x = \alpha$, we have:

$$[\beta] = \beta^+ - \beta^- \geq 0. \quad (4.3)$$

For simplicity, we assume that $2\beta^- - \sigma^2 > 0$. The jump conditions at $x = \alpha$ are

$$[u] = u_1, \quad (4.4)$$

$$\left[\beta \frac{\partial u}{\partial x} \right] = u_2. \quad (4.5)$$

We consider this problem with Neumann boundary condition

$$\frac{\partial u}{\partial x} \Big|_{x=0} = a, \quad \frac{\partial u}{\partial x} \Big|_{x=1} = b. \quad (4.6)$$

In this problem, we only have Neumann boundary conditions. As we know, in the previous Poisson problems, we need additional conditions to guarantee that the problems with Neumann boundary conditions have unique solutions. But in this problem, no additional condition is needed. We start with reviewing the finite difference scheme from the immersed interface method (IIM).

4.1 Review of the IIM

To apply the finite difference method to this problem, we generate a Cartesian grid with step size h in the interval $[0, 1]$. $x = \alpha$ is the interface. We assume that $x_j < \alpha < x_{j+1}$. Thus, we have the finite difference scheme

$$L_h U_i = \gamma_{i,1} U_{i-1} + \gamma_{i,2} U_i + \gamma_{i,3} U_{i+1} = f_i, \quad (4.7)$$

where $\gamma_{i,1}$, $\gamma_{i,2}$ and $\gamma_{i,3}$ are coefficients to be determined, U_i is the numerical solution to the value of $u(x)$ at point $x = x_i$, and f_i is the value of $f(x)$ at $x = x_i$.

According to the method to determine the coefficients in [22], we have the coefficients in the scheme (4.7) at regular points

$$\begin{cases} \gamma_{i,1} = \frac{\beta}{h^2}, \\ \gamma_{i,2} = -\frac{2\beta}{h^2} - \sigma^2, \\ \gamma_{i,3} = \frac{\beta}{h^2}. \end{cases} \quad (4.8)$$

At the irregular point x_j , the coefficients are

$$\begin{cases} \gamma_{j,1} = \frac{\beta^- - [\beta](x_j - \alpha)/h}{D_j}, \\ \gamma_{j,2} = \frac{-2\beta^- + [\beta](x_{j-1} - \alpha)/h}{D_j} - \sigma^2, \\ \gamma_{j,3} = \frac{\beta^+}{D_j}, \end{cases} \quad (4.9)$$

where

$$D_j = h^2 + \frac{[\beta](\alpha - x_{j-1})(\alpha - x_j)}{2\beta^-}. \quad (4.10)$$

And at the irregular point x_{j+1} , the coefficients are

$$\begin{cases} \gamma_{j+1,1} = \frac{\beta^-}{D_{j+1}}, \\ \gamma_{j+1,2} = \frac{-2\beta^+ + [\beta](x_{j+2} - \alpha)/h}{D_{j+1}} - \sigma^2, \\ \gamma_{j+1,3} = \frac{\beta^+ - [\beta](x_{j+1} - \alpha)/h}{D_{j+1}}, \end{cases} \quad (4.11)$$

where

$$D_{j+1} = h^2 - \frac{[\beta](x_{j+2} - \alpha)(x_{j+1} - \alpha)}{2\beta^+}. \quad (4.12)$$

With these coefficients determined, if we write the linear system of numerical solution into matrix form. The matrix of coefficients is a tri-diagonal matrix. But the difference between the matrix of this problem and the matrix of the Poisson equation we mentioned previously is that the matrix for this problem is more diagonal dominant. This implies that the matrix of coefficients is invertible. Thus, when we solve the linear system of numerical solution, the solution is unique. And no additional condition is needed. With the problem well-posed, in the rest of this chapter, we will use the method from the maximum principle and related theorems to show our result of the immersed interface method for the problem. The most important part is finding a comparison function.

4.2 A comparison function

To apply the method from the maximum principle and related theorems in [16], a comparison function $\Phi(x)$ is needed. The comparison function should satisfy that it is non-negative and $L_h\Phi(x) \geq C_1 > 0$ where L_h is the finite difference scheme (4.7). We claim the comparison function

$$\Phi(x) = \begin{cases} \frac{1}{\beta^-}(x - \alpha)^2 + \frac{1}{\beta^-}(x_j - x)^2, & x \leq \alpha, \\ \frac{1}{\beta^+}(x - \alpha)^2 + \frac{1}{\beta^+}(x - x_{j+1})^2, & x > \alpha. \end{cases} \quad (4.13)$$

Because $\beta(x)$ is positive. For $x \in \Omega$, $\Phi(x) > 0$. When we apply the finite difference stencil L_h to the comparison function $\Phi(x)$.

At regular point x_i , we assume that $x_{i-1} < x_i < x_{i+1} < \alpha$. We have

$$\begin{aligned}
L_h\Phi(x_i) &= \gamma_{j,1}\Phi(x_{i-1}) + \gamma_{j,2}\Phi(x_i) + \gamma_{j,2}\Phi(x_{i+1}) \\
&= 4 - \frac{\sigma^2}{\beta^-}(x_i - \alpha)^2 - \frac{\sigma^2}{\beta^-}(x_i - x_j)^2 \\
&\geq 4 - \frac{2\sigma^2}{\beta^-} > C_1 > 0,
\end{aligned} \tag{4.14}$$

because we have $2\beta^- - \sigma^2 > 0$, $(x_i - \alpha)^2 < 1$ and $(x_i - x_j)^2 < 1$.

For $\alpha < x_{i-1} < x_i < x_{i+1}$, we have

$$\begin{aligned}
L_h\Phi(x_i) &= 4 - \frac{\sigma^2}{\beta^+}(x_i - \alpha)^2 - \frac{\sigma^2}{\beta^+}(x_i - x_{j+1})^2 \\
&\geq 4 - \frac{2\sigma^2}{\beta^+} > C_1 > 0,
\end{aligned} \tag{4.15}$$

because $\beta^+ \geq \beta^-$ such that $2\beta^+ - \sigma^2 > 2\beta^- - \sigma^2 > 0$.

At irregular point x_j , we have $x_{j-1} < x_j < \alpha < x_{j+1}$. We have already had the coefficients of scheme from (4.9).

And $\Phi(x)$ at x_{j-1} , x_j and x_{j+1} are

$$\Phi(x_{j-1}) = \frac{1}{\beta^-}(x_{j-1} - \alpha)^2 + \frac{1}{\beta^-}(x_j - x_{j-1})^2, \tag{4.16}$$

$$\Phi(x_j) = \frac{1}{\beta^-}(x_j - \alpha)^2, \tag{4.17}$$

$$\Phi(x_{j+1}) = \frac{1}{\beta^+}(x_{j+1} - \alpha)^2. \tag{4.18}$$

Then we plug them into $L_h\Phi(x_i) = \gamma_{j,1}\Phi(x_{j-1}) + \gamma_{j,2}\Phi(x_j) + \gamma_{j,3}\Phi(x_{j+1})$. We have

$$\begin{aligned}
L_h\Phi(x_i) &= \frac{2\beta^-h^2}{D_j\beta^-} + \frac{\beta^-h^2}{D_j\beta^-} + \frac{[\beta](x_j - \alpha)(x_{j-1} - \alpha)}{D_j\beta^-} - \frac{[\beta](x_j - \alpha)h}{D_j\beta^-} - \frac{\sigma^2}{\beta^-}(x_i - \alpha)^2 \\
&= \frac{2\beta^-h^2 + \beta^-h^2 + [\beta](x_j - \alpha)(x_{j-2} - \alpha)}{\beta^- \left(h^2 + \frac{[\beta](\alpha - x_{j-1})(\alpha - x_j)}{2\beta^-} \right)} - \frac{\sigma^2}{\beta^-}(x_j - \alpha)^2 \\
&\geq \frac{2\beta^-h^2 + \beta^-h^2 + [\beta](x_j - \alpha)(x_{j-2} - \alpha) - \left(h^2 + \frac{[\beta](x_{j-1} - \alpha)(x_j - \alpha)}{2\beta^-} \right) \sigma^2}{\beta^- \left(h^2 + \frac{[\beta](\alpha - x_{j-1})(\alpha - x_j)}{2\beta^-} \right)} \\
&\geq \frac{(2\beta^- - \sigma^2)h^2 + \beta^-h^2 + [\beta](x_j - \alpha) \left((x_{j-2} - \alpha) - \frac{\sigma^2(x_{j-1} - \alpha)}{2\beta^-} \right)}{\beta^- \left(h^2 + \frac{[\beta]h^2}{2\beta^-} \right)} \\
&\geq \frac{(2\beta^- - \sigma^2)h^2 + \beta^-h^2 + [\beta]\frac{\sigma^2}{2\beta^-}(\alpha - x_j)h}{\beta^- \left(h^2 + \frac{[\beta]h^2}{2\beta^-} \right)} \\
&\geq O(1) + \frac{C_2}{h},
\end{aligned} \tag{4.19}$$

because we have $2\beta^- - \sigma^2 > 0$. And C_2 is determined by jumps of $\beta(x)$ and σ .

For irregular points $x_{j+1} > \alpha$, we can have the result in the same way

$$L_h\Phi(x_{j+1}) \geq O(1) + \frac{C_2}{h}. \tag{4.20}$$

From above, we conclude

$$L_h\Phi(x_i) \begin{cases} \geq 4 - \frac{2\sigma^2}{\beta^-}, & 0 < x_i < x_j, \\ \geq 4 - \frac{2\sigma^2}{\beta^+}, & x_{j+1} < x_i < 1, \\ \geq O(1) + \frac{C_2}{h}, & x_i = x_j \quad \text{or} \quad x_i = x_{j+1}. \end{cases} \quad (4.21)$$

With the comparison function, we have our result for the problem (4.1), (4.4), (4.6).

4.3 Main convergence result

In this section, we claim the result of error analysis:

Theorem 4.3.1. *We consider the problem with Neumann boundary condition (4.1), (4.4), (4.6). And we assume that $2\beta^- - \sigma^2 > 0$. We use the finite difference stencil L_h such that it has a unique solution. Let $u^e \in C^3$ be the exact solution to this problem. And u^h is the numerical solution. Then the estimation of error of numerical solution obtained from immersed interface method is bounded as follows*

$$\|u^h - u^e\| \leq Ch^2, \quad (4.22)$$

where C is the constant depend on $\beta(x)$ and σ .

Proof. To prove this theorem, we use the non-negative comparison function (4.13). Ap-

plying the finite difference stencil L_h to the comparison function, we have

$$L_h\Phi(x_i) \begin{cases} \geq 4 - \frac{2\sigma^2}{\beta^-}, & 0 < x_i < x_j, \\ \geq 4 - \frac{2\sigma^2}{\beta^+}, & x_{j+1} < x_i < 1, \\ \geq O(1) + \frac{C_2}{h}, & x_i = x_j \quad \text{or} \quad x_i = x_{j+1}. \end{cases} \quad (4.23)$$

We also know that at regular points, the truncation error $|T(x_i)|$ is bounded by

$$|T(x_i)| < C_3h^2, \quad (4.24)$$

such that

$$\frac{|T(x_i)|}{L_h\Phi(x_i)} \leq \frac{C_3h^2}{C_1}. \quad (4.25)$$

And at irregular points, the truncation error $|T(x_i)|$ is bounded by

$$|T(x_i)| < C_4h, \quad (4.26)$$

such that

$$\frac{|T(x_i)|}{L_h\Phi(x_i)} \leq \frac{C_4h}{C_2/h} = \frac{C_4h^2}{C_2}. \quad (4.27)$$

At points $x = 0$ and $x = 1$, we have the value of $\Phi(x)$

$$\Phi(0) = \frac{1}{\beta^-}\alpha^2 + \frac{1}{\beta^-}x_j^2, \quad (4.28)$$

$$\Phi(1) = \frac{1}{\beta^+}(1 - \alpha)^2 + \frac{1}{\beta^+}(1 - x_{j+1})^2. \quad (4.29)$$

The value on the boundary are finite. From the result of Lemma 3.1.5, the global

error of numerical solution obtained from the immersed interface method is bounded as follows

$$\|u^h - u^e\| \leq Ch^2, \tag{4.30}$$

which means that the numerical solution is second-order accurate. □

4.4 Conclusion

In this section, we consider the elliptic problem (4.1), (4.4), (4.6) with an interface and Neumann boundary conditions. But this problem does not need additional conditions to guarantee the problem well-posed. By constructing a non-negative comparison function, we estimate the positive low bounds for $L_h\Phi$ at regular and irregular points such that we can use the Lemma 3.1.5 from the maximum principle to give Theorem 4.3.1.

Chapter 5

ERROR ANALYSIS OF THE IMMERSED INTERFACE METHOD FOR THE INCOMPRESSIBLE STOKES EQUATIONS WITH AN INTERFACE

In this chapter, we consider the Stokes equations on a rectangular domain Ω with an interface Γ

$$\nabla p = \mu \Delta \mathbf{u} + F + \mathbf{g}, \quad \mathbf{x} \in \Omega, \quad (5.1)$$

$$\nabla \cdot \mathbf{u} = 0, \tag{5.2}$$

where \mathbf{u} is the velocity, p is pressure, \mathbf{g} is a body force, and F is a source distribution along a closed smooth interface $\Gamma \in \Omega$ as in Peskin's immersed boundary (IB) model [23],

$$F(\mathbf{x}) = \int_{\Gamma} f(s) \delta_2(\mathbf{x} - \mathbf{X}(s)) ds, \tag{5.3}$$

where δ_2 is the Dirac delta function in two dimensional space.

We recall the Figure 2.1 in Chapter 2 as illustration.

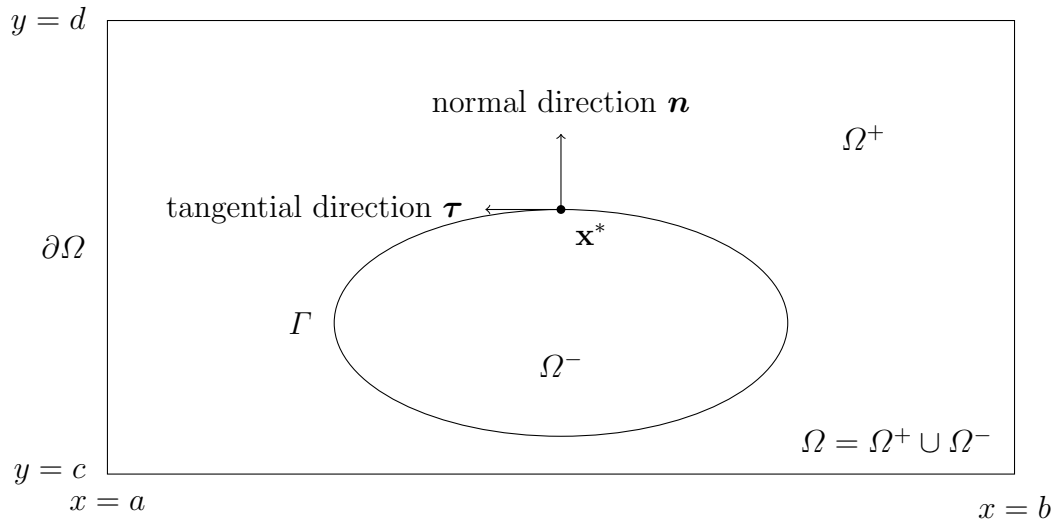


Figure 5.1 A diagram of an interface Γ in the domain Ω , with the tangential $\boldsymbol{\tau}$ and normal direction \mathbf{n} at a point \mathbf{x}^* on the interface.

Because of the presence of the singular source, the pressure and its normal derivative, and the normal derivative of the velocity are discontinuous across the interface. The jump

relations below

$$[p] = \hat{f}_1, \quad (5.4)$$

$$\left[\frac{\partial p}{\partial n} \right] = \frac{\partial}{\partial \tau} \hat{f}_2, \quad (5.5)$$

$$\left[\frac{\partial \mathbf{u}}{\partial n} \cdot \boldsymbol{\tau} \right] + \left[\frac{\partial \mathbf{u}}{\partial \tau} \cdot \mathbf{n} \right] + \hat{f}_2 = 0, \quad (5.6)$$

$$[\nabla \cdot \mathbf{u}] = 0, \quad (5.7)$$

are derived in [21], where $\hat{f}_1 = f \cdot \mathbf{n}$ and $\hat{f}_2 = f \cdot \boldsymbol{\tau}$. The definition of jump condition has been defined in Chapter 2.

There are variety of numerical methods for solving the Stokes interface problems. Among them, the immersed interface method using three Poisson equations approach [22] may be one of the most efficient if the pressure boundary condition can be taken care of¹. In the three Poisson equations approach, assuming that the viscosity is a constant in the entire domain, then by applying the divergence operator to the momentum equation (5.1), we get a Poisson equation across the interface for the pressure with the known jump condition in the normal derivative. After we have computed the pressure, we can solve two Poisson equations again to get the velocity from the momentum equation. Advantages of this approach is that we can solve each Poisson equation using a fast Poisson solver such as the Fishpack [10] which makes the method very efficient and fast. The three Poisson equations approach is also the basis for the augmented Stokes solver for problems with discontinuous viscosity in [33].

While the three Poisson equations approach seems to provide second-order accurate

¹It is easier to deal with periodic boundary conditions for all the variables which is not discussed here.

pressure and velocity. Rigorous proof is still missing up to today. This is the main motivation of this chapter to provide such convergence proof. Note that, when the IIM is applied to solve a Poisson equations with known jump conditions in the normal derivative, the local truncation error is $O(h^2)$ at regular grid points and it is $O(h)$ at irregular grid points where the interface cuts through the standard centered five-point stencil, where h is the mesh size. Nevertheless, the global error is $O(h^2)$ in the infinity norm. In [2], it shows second order convergence for the solution for the velocity, but not for the pressure. In this chapter, we provide a proof for the pressure which has a Neumann boundary condition. To simplify the Neumann boundary condition for pressure, we assume that $\Delta u = O(h)$ at the boundary of Ω .

In the following of this chapter, we are going to review the three Poisson equations approach and its equivalence to the original formulation in Section 5.1. In Section 5.2, we show main results for the Stokes equations and recall the lemmas in Chapter 2 to help prove the results. In Section 5.4, we show the second order convergency for the velocity Poisson equations. We conclude in the last section.

5.1 Review of the three Poisson equations approach

We consider the Stokes equations with constant viscosity μ . For simplicity we assume $\mu = 1$. Then (5.1), (5.2) are simplified

$$\nabla p = \Delta \mathbf{u} + F + \mathbf{g}, \quad \mathbf{x} \in \Omega, \quad (5.8)$$

$$\nabla \cdot \mathbf{u} = 0, \quad (5.9)$$

where p is piecewise C^1 , \mathbf{u} is piece-wise C^2 . We assume that p and $\mathbf{u} = (u, v)^\top$ are smooth in each subdomain Ω_- and Ω_+ . After decoupling the Stokes equations, three Poisson equations are provided. To preserve velocity divergence-free, a Neumann boundary condition of pressure can be claimed. Thus, the Poisson equations for pressure should be combined with a Neumann boundary condition. We cannot apply the result from [2] to it.

By applying divergence on the equation $\nabla p = \Delta \mathbf{u} + F + \mathbf{g}$, we can decouple the velocity and pressure. After decoupling, we not only decouple the equations, but also decouple the jump conditions on interface. Thus, we have three Poisson equations with jump conditions

$$\Delta p = \nabla \cdot (F + \mathbf{g}), \quad (5.10)$$

$$[p] = \hat{f}_1, \quad (5.11)$$

$$\left[\frac{\partial p}{\partial n} \right] = \frac{\partial}{\partial \tau} \hat{f}_2, \quad (5.12)$$

$$\Delta u = p_x - (F_1 + g_1), \quad (5.13)$$

$$\left[\frac{\partial u}{\partial n} \right] = \hat{f}_2 \sin \theta, \quad (5.14)$$

$$\Delta v = p_y - (F_2 + g_2), \quad (5.15)$$

$$\left[\frac{\partial v}{\partial n} \right] = -\hat{f}_2 \cos \theta, \quad (5.16)$$

$$[u] = 0, [v] = 0, \quad (5.17)$$

where θ is the angle between normal direction of the interface and horizontal axis, $\mathbf{g} = (g_1, g_2)^\top$ and $F = (F_1, F_2)^\top$.

For pressure, we have

$$\Delta p = \nabla \cdot (F + \mathbf{g}), \quad (5.18)$$

$$[p] = \hat{f}_1, \quad (5.19)$$

$$\left[\frac{\partial p}{\partial n} \right] = \frac{\partial}{\partial \tau} \hat{f}_2. \quad (5.20)$$

Then we apply immersed interface method [17, 22] to these equations to solve pressure.

From [14], when we apply divergence to the Stokes equations for decoupling, we need to make sure that the velocity \mathbf{u} is still divergence-free after decoupling. A Neumann boundary condition for pressure can be derived. In next subsections, we review the derivation of Neumann boundary condition and prove the divergence-free of velocity. For simplicity, we call $F + \mathbf{g} = G$.

5.1.1 Neumann boundary condition for the pressure

We claim the following Neumann boundary condition [13, 14] for pressure

$$\frac{\partial p}{\partial n} \Big|_{\partial\Omega} = [-\mathbf{n} \cdot (\nabla \times \nabla \times \mathbf{u}) + \mathbf{n} \cdot G] \Big|_{\partial\Omega}, \quad (5.21)$$

where \mathbf{n} is a unit normal vector along $\partial\Omega$. A new system equivalent to the original Stokes equations is given by

$$\Delta \mathbf{u} = \nabla p - G, \quad (5.22)$$

$$\frac{\partial p}{\partial n} \Big|_{\partial\Omega} = [-\mathbf{n} \cdot (\nabla \times \nabla \times \mathbf{u}) + \mathbf{n} \cdot G] \Big|_{\partial\Omega}, \quad (5.23)$$

$$\mathbf{u} \Big|_{\partial\Omega} = 0. \quad (5.24)$$

Next, we will prove the equivalence between the given system and the origin system.

5.1.2 Proof of the equivalence and the divergence-free of velocity

Recall the vector identity

$$\Delta \mathbf{u} = -\nabla \times \nabla \times \mathbf{u} + \nabla(\nabla \cdot \mathbf{u}). \quad (5.25)$$

Along the boundary $\partial\Omega$, take inner product of $\nabla p = \Delta \mathbf{u} + G$ and \mathbf{n} . Then replace $\Delta \mathbf{u}$ by $-\nabla \times \nabla \times \mathbf{u} + \nabla(\nabla \cdot \mathbf{u})$,

$$\left. \frac{\partial p}{\partial n} \right|_{\partial\Omega} = \left[-\mathbf{n} \cdot (\nabla \times \nabla \times \mathbf{u}) + \frac{\partial(\nabla \cdot \mathbf{u})}{\partial n} + \mathbf{n} \cdot G \right] \Big|_{\partial\Omega}. \quad (5.26)$$

Comparing with

$$\left. \frac{\partial p}{\partial n} \right|_{\partial\Omega} = \left[-\mathbf{n} \cdot (\nabla \times \nabla \times \mathbf{u}) + \mathbf{n} \cdot G \right] \Big|_{\partial\Omega}, \quad (5.27)$$

we have

$$\left. \frac{\partial(\nabla \cdot \mathbf{u})}{\partial n} \right|_{\partial\Omega} = 0. \quad (5.28)$$

From [14], set $\phi = \nabla \cdot \mathbf{u}$. From previous information, we have equations

$$\left\{ \begin{array}{l} \Delta \phi = 0, \\ \left. \frac{\partial \phi}{\partial n} \right|_{\partial\Omega} = 0, \\ \phi(0) = 0. \end{array} \right. \quad (5.29)$$

Then solve this PDEs using separation of variables [15].

$$\phi = \nabla \cdot \mathbf{u} = 0. \quad (5.30)$$

This means that with the Neumann boundary condition for pressure, the divergence-free of velocity still holds after decoupling. The Poisson equations for pressure with a Neumann boundary condition can be written as

$$\Delta p = \nabla \cdot G = F, \quad (5.31)$$

$$\left. \frac{\partial p}{\partial n} \right|_{\partial\Omega} = [-\mathbf{n} \cdot (\nabla \times \nabla \times \mathbf{u}) + \mathbf{n} \cdot G]_{\partial\Omega}, \quad (5.32)$$

$$[p] = \hat{f}_1, \quad (5.33)$$

$$\left[\frac{\partial p}{\partial n} \right] = \frac{\partial}{\partial \tau} \hat{f}_2. \quad (5.34)$$

With the vector identity (5.25), we can write the Neumann boundary condition into

$$\left. \frac{\partial p}{\partial n} \right|_{\partial\Omega} = [\mathbf{n} \cdot (\Delta \mathbf{u}) + \mathbf{n} \cdot G]_{\partial\Omega}. \quad (5.35)$$

With the Neumann boundary condition of pressure, in next section, we show results for the Stokes equations.

5.2 Main convergence results

In the rest of this chapter, we follow the notations in Chapter 2. For the Poisson problem of pressure:

$$\Delta p = \nabla \cdot G = F, \quad (5.36)$$

$$\left. \frac{\partial p}{\partial n} \right|_{\partial\Omega} = [\mathbf{n} \cdot \Delta u + \mathbf{n} \cdot G]_{\partial\Omega}, \quad (5.37)$$

$$[p] = \hat{f}_1, \quad (5.38)$$

$$\left[\frac{\partial p}{\partial n} \right] = \frac{\partial}{\partial \tau} \hat{f}_2. \quad (5.39)$$

Recall definitions of regular and irregular points in Chapter 2. Let p^e be the exact solution. At regular grid points we have the truncation error

$$\Delta_h p^e(\mathbf{j}h) = F_{\pm}(\mathbf{j}h) + \tau^h(\mathbf{j}h), \quad \|\tau^h(\mathbf{j}h)\| \leq Ch^2, \quad (5.40)$$

where F_{\pm} is based on whether $\mathbf{j}h \in \Omega_+$ or Ω_- . Then we consider the truncation error at irregular points, we have $T^h(\mathbf{j}h)$, determined by jumps on Γ . So that

$$\Delta_h p^e(\mathbf{j}h) = F_{\pm}(\mathbf{j}h) + T^h(\mathbf{j}h) + \tau^h(\mathbf{j}h), \quad \|\tau^h(\mathbf{j}h)\| \leq Ch. \quad (5.41)$$

We define F^h on Ω_h by

$$F^h(\mathbf{j}h) = \begin{cases} F_{\pm}(\mathbf{j}h) + T^h(\mathbf{j}h), & \mathbf{j}h \text{ irregular,} \\ F_{\pm}(\mathbf{j}h), & \mathbf{j}h \text{ regular.} \end{cases} \quad (5.42)$$

Thus, we can have p^h as the solution to

$$\Delta_h p^h = F^h \quad \text{in } \Omega_h, \quad D^+ p^h = \mathbf{n} \cdot \Delta u + \mathbf{n} \cdot G \quad \text{on } \partial\Omega_h, \quad (5.43)$$

where $D^+ p^h$ is the central difference stencil which we have defined in Chapter 2 on the boundary.

Then, with assumption $\Delta u = O(h)$ on $\partial\Omega$, the error $p^h - p^e$ will satisfy

$$\Delta_h(p^h - p^e) = -\tau^h \quad \text{in } \Omega_h, \quad D^+(p^h - p^e) = O(h) \quad \text{on } \partial\Omega_h. \quad (5.44)$$

After the preparation above, we can state our results with a Neumann boundary condition which is different from the result in [2]. After the theorem and related lemmas, proofs will be given. The theorem implies that the error in (2.19) is uniformly $O(h^2)$, although the local truncation errors are $O(h)$ at irregular grid points in Ω :

Theorem 5.2.1. *Let p^e be the exact solution of pressure in Stokes equations (5.1), (5.2) with the interface Γ at least C^1 . Suppose $\Delta_h p^e$ has the form given by (5.40), (5.41), with $\|\tau_h(\mathbf{j}h)\| \leq Ch$ at irregular grid points and $\|\tau_h(\mathbf{j}h)\| \leq Ch^2$ at regular grid points. Let p^h be the solution to (5.42), (5.43). Assume that there is a chosen grid point (α, β) , where $p^h - p^e = 0$. Then,*

$$\|p^h - p^e\|_{\bar{\Omega}_h} = O(h^2), \quad (5.45)$$

and

$$\|D_1^+(p^h - p^e)\|_{\bar{\Omega}_h} = O(h^2), \quad (5.46)$$

$$\|D_2^+(p^h - p^e)\|_{\bar{\Omega}_h} = O(h^2). \quad (5.47)$$

Meanwhile, the errors between exact solutions and computational solutions to velocity $\mathbf{u} = (u, v)^\top$ are

$$|u^h - u^e| = O(h^2), \quad (5.48)$$

$$|v^h - v^e| = O(h^2). \quad (5.49)$$

The estimations of $\|D_1^+(p^h - p^e)\|_{\overline{\Omega}_h}$ and $\|D_2^+(p^h - p^e)\|_{\overline{\Omega}_h}$ will be derived in Section 5.4. And **Theorem 5.2.1** can be proved with the next three lemmas, which are proved in Section 5.3.

To prove the **Theorem 5.2.1**, we will use the **Lemma 2.3.2** in Chapter 2. And we also need a lemma which is similar to lemma 2.3.3:

Lemma 5.2.2. *Suppose*

$$\Delta_h v = F^{reg} + D_1^- F_1 + D_2^- F_2 \quad \text{in } \Omega_h, \quad D^+ v = -O(h) \quad \text{on } \partial\Omega_h. \quad (5.50)$$

Then

$$\begin{aligned} \|\nabla_h^+ v\|_{\overline{\Omega}_h}^2 &\leq \|F^{reg}\|_{\overline{\Omega}_h} \|v\|_{\overline{\Omega}_h} + (\|F_1\|_{\overline{\Omega}_h} + O(h^3)) \|D_1^+ v\|_{\overline{\Omega}_h} \\ &\quad + (\|F_2\|_{\overline{\Omega}_h} + O(h^3)) \|D_2^+ v\|_{\overline{\Omega}_h} + 4O(h^2) \|v\|_{\overline{\Omega}_h}, \end{aligned} \quad (5.51)$$

where F^{reg} is a function on the set of regular points.

Recall the discrete Neumann-Poincare inequality (Lemma 2.3.4):

Lemma 5.2.3 (Discrete Neumann-Poincare inequality). *If v is C^1 on Ω_h , we define*

$$A = v(c_1, c_2), \quad (5.52)$$

where (c_1, c_2) is a point on Ω_h .

Then,

$$\|v - A\|_{\overline{\Omega}_h} \leq C \|\nabla_h^+ v\|_{\overline{\Omega}_h}. \quad (5.53)$$

To derive the Theorem, we set F^{irr} equal to the restriction of τ^h at those irregular points and use Lemma 2.3.2 so that $F_1 = O(h^2)$ and $F_2 = O(h^2)$. We apply Lemma 5.2.2 to $v = p^h - p^e$,² using (5.44) with F^{reg} equal to the regular part of τ^h . To make the Stokes equation compatible, give a chosen point (α, β) where $v = 0$. We can set A in Lemma 2.3.4 as the error of pressure at point (α, β) . Combing (5.51) with Lemma 2.3.4, the second order accuracy error can be derived.

In order to derive (5.46) and (5.47) in the Theorem 5.2.1, we will use the result of Lemma 5.2.2. During the derivation, we need to discuss whether $D_1^+(p^h - p^e)$ and $D_2^+(p^h - p^e)$ are zeros. But the different situations won't affect the result. The detail will be explained later.

In next section, we will see the proofs of Theorem 5.2.1 and Lemma 5.2.2.

5.3 Proofs of theorem 5.2.1 and the lemma 5.2.2

Proof of Lemma 5.2.2. Similar to the proof of Lemma 2.3.3, we multiply by v in (5.50), sum over Ω_h and then sum by parts on the left, using the Neumann boundary condition for v

$$(\Delta_h v, v)_{\overline{\Omega}_h} = \sum_{jh \in \overline{\Omega}_h} (D_1^- D_1^+ v + D_2^- D_2^+ v) v h^2$$

²The v here is not the one in velocity. It represent the error of pressure here.

$$\begin{aligned}
&= \sum_{jh \in \overline{\Omega}_h} D_1^- D_1^+ v \cdot v h^2 + \sum_{jh \in \overline{\Omega}_h} D_2^- D_2^+ v \cdot v h^2 \\
&= - \sum_{jh \in \overline{\Omega}_h} [(D_1^+ v)^2 + (D_2^+ v)^2] h^2 \\
&+ \sum_{j_2=0}^M [D_1^+ v(Nh, j_2h)]^2 \cdot h^2 + \sum_{j_1=0}^N [D_2^+ v(j_1h, Mh)]^2 \cdot h^2 \quad (5.54) \\
&- \sum_{j_2=0}^M D_1^+ v(0, j_2h) \cdot v(0, j_2h) \cdot h \\
&- \sum_{j_1=0}^N D_2^+ v(j_1h, 0) \cdot v(j_1h, 0) \cdot h \\
&+ \sum_{j_2=0}^M D_1^+ v(Nh, j_2h) \cdot v(Nh, j_2h) \cdot h \\
&+ \sum_{j_1=0}^N D_2^+ v(j_1h, Mh) \cdot v(j_1h, Mh) \cdot h.
\end{aligned}$$

$$\begin{aligned}
(\Delta_h v, v)_{\overline{\Omega}_h} &= -(\nabla_h^+ v, \nabla_h^+ v)_{\overline{\Omega}_h} \\
&+ \sum_{j_2=0}^M [D_1^+ v(Nh, j_2h)]^2 \cdot h^2 + \sum_{j_1=0}^N [D_2^+ v(j_1h, Mh)]^2 \cdot h^2 \\
&- \sum_{j_2=0}^M D_1^+ v(0, j_2h) \cdot v(0, j_2h) \cdot h \quad (5.55) \\
&- \sum_{j_1=0}^N D_2^+ v(j_1h, 0) \cdot v(j_1h, 0) \cdot h \\
&+ \sum_{j_2=0}^M D_1^+ v(Nh, j_2h) \cdot v(Nh, j_2h) \cdot h
\end{aligned}$$

$$+ \sum_{j_1=0}^N D_2^+ v(j_1 h, Mh) \cdot v(j_1 h, Mh) \cdot h.$$

On the right hand side,

$$\begin{aligned} (F^{reg} + D_1^- F_1 + D_2^- F_2, v)_{\overline{\Omega}_h} &= (F^{reg}, v)_{\overline{\Omega}_h} \\ &+ (D_1^- F_1, v)_{\overline{\Omega}_h} + (D_2^- F_2, v)_{\overline{\Omega}_h}. \end{aligned} \quad (5.56)$$

Consider $(D_1^- F_1, v)$ and use summation by parts with $F_1 = 0$ on the boundary,

$$\begin{aligned} (D_1^- F_1, v)_{\overline{\Omega}_h} &= \sum_{jh \in \overline{\Omega}_h} D_1^- F_1(j_1 h, j_2 h) v(j_1 h, j_2 h) h^2 \\ &= \sum_{jh \in \overline{\Omega}_h} [F_1(j_1 h, j_2 h) - F_1((j_1 - 1)h, j_2 h)] v(j_1 h, j_2 h) h \\ &= -(F_1, D_1^+ v) + \sum_{j_2=0}^M F_1(Nh, j_2 h) D_1^+ v(Nh, j_2 h) h^2 \\ &\quad - \sum_{j_2=0}^M F_1(0, j_2 h) v(0, j_2 h) h + \sum_{j_2=0}^M F_1(Nh, j_2 h) v(Nh, j_2 h) h \\ &= -(F_1, D_1^+ v)_{\overline{\Omega}_h}. \end{aligned} \quad (5.57)$$

Similarly, we have

$$(D_2^- F_2, v)_{\overline{\Omega}_h} = -(F_2, D_2^+ v)_{\overline{\Omega}_h}. \quad (5.58)$$

Thus,

$$\begin{aligned} (F^{reg} + D_1^- F_1 + D_2^- F_2, v)_{\overline{\Omega}_h} &= (F^{reg}, v)_{\overline{\Omega}_h} \\ &- (F_1, D_1^+ v)_{\overline{\Omega}_h} - (F_2, D_2^+ v)_{\overline{\Omega}_h}. \end{aligned} \quad (5.59)$$

Combining $(\Delta_h v, v)_{\overline{\Omega}_h}$ with $(F^{reg} + D_1^- F_1 + D_2^- F_2, v)_{\overline{\Omega}_h}$, we have

$$\begin{aligned}
(F^{reg}, v)_{\overline{\Omega}_h} - (F_1, D_1^+ v)_{\overline{\Omega}_h} - (F_2, D_2^+ v)_{\overline{\Omega}_h} &= -(\nabla_h^+ v, \nabla_h^+ v)_{\overline{\Omega}_h} \\
&+ \sum_{j_2=0}^M [D_1^+ v(Nh, j_2h)]^2 \cdot h^2 + \sum_{j_1=0}^N [D_2^+ v(j_1h, Mh)]^2 \cdot h^2 \\
&- \sum_{j_2=0}^M D_1^+ v(0, j_2h) \cdot v(0, j_2h) \cdot h \\
&- \sum_{j_1=0}^N D_2^+ v(j_1h, 0) \cdot v(j_1h, 0) \cdot h \\
&+ \sum_{j_2=0}^M D_1^+ v(Nh, j_2h) \cdot v(Nh, j_2h) \cdot h \\
&+ \sum_{j_1=0}^N D_2^+ v(j_1h, Mh) \cdot v(j_1h, Mh) \cdot h.
\end{aligned} \tag{5.60}$$

As we know, we have defined D_1^+ and D_2^+ on the boundary. We have

$$D_1^+ v = -O(h), D_2^+ v = -O(h) \quad \text{on the boundary.} \tag{5.61}$$

Thus, using Cauchy-Schwarz inequality we can have inequality

$$\begin{aligned}
\|\nabla_h^+ v\|_{\overline{\Omega}_h}^2 &\leq \|F^{reg}\|_{\overline{\Omega}_h} \|v\|_{\overline{\Omega}_h} + (\|F_1\|_{\overline{\Omega}_h} + O(h^3)) \|D_1^+ v\|_{\overline{\Omega}_h} \\
&+ (\|F_2\|_{\overline{\Omega}_h} + O(h^3)) \|D_2^+ v\|_{\overline{\Omega}_h} + 4O(h^2) \|v\|_{\overline{\Omega}_h}.
\end{aligned} \tag{5.62}$$

□

With Lemma 5.2.2 and Lemma 2.3.4, we can derive the pressure part of Theorem 5.2.1.

Proof of Theorem 5.2.1. In this proof, we only prove the result of pressure in Theorem

5.2.1. The proof of the results for velocities will be shown in later section. To make sure that the boundary value problem of pressure has a unique solution we have $v(\alpha, \beta) = 0$. We set $A = v(\alpha, \beta) = 0$. Then the inequality will become

$$\|v\|_{\bar{\Omega}_h} \leq C\|\nabla_h^+ v\|_{\bar{\Omega}_h}. \quad (5.63)$$

Back to the inequality 5.51 in Lemma 5.2.2

$$\begin{aligned} \|\nabla_h^+ v\|_{\bar{\Omega}_h}^2 &\leq \|F^{reg}\|_{\bar{\Omega}_h} \|v\|_{\bar{\Omega}_h} + (\|F_1\|_{\bar{\Omega}_h} + O(h^3)) \|D_1^+ v\|_{\bar{\Omega}_h} \\ &\quad + (\|F_2\|_{\bar{\Omega}_h} + O(h^3)) \|D_2^+ v\|_{\bar{\Omega}_h} + 4O(h^2) \|v\|_{\bar{\Omega}_h}. \end{aligned} \quad (5.64)$$

With the discrete Neumann-Poincare inequality, we can have

$$\begin{aligned} \|\nabla_h^+ v\|_{\bar{\Omega}_h}^2 &\leq C\|F^{reg}\|_{\bar{\Omega}_h} \|\nabla_h^+ v\|_{\bar{\Omega}_h} + (\|F_1\|_{\bar{\Omega}_h} + O(h^3)) \|\nabla_h^+ v\|_{\bar{\Omega}_h} \\ &\quad + (\|F_2\|_{\bar{\Omega}_h} + O(h^3)) \|\nabla_h^+ v\|_{\bar{\Omega}_h} + 4CO(h^2) \|\nabla_h^+ v\|_{\bar{\Omega}_h}. \end{aligned} \quad (5.65)$$

Divided by $\|\nabla_h^+ v\|_{\bar{\Omega}_h}$ on the both sides

$$\begin{aligned} \|v\|_{\bar{\Omega}_h} &\leq C\|\nabla_h^+ v\|_{\bar{\Omega}_h} \leq C^2\|F^{reg}\|_{\bar{\Omega}_h} + C(\|F_1\|_{\bar{\Omega}_h} + O(h^3)) \\ &\quad + C(\|F_2\|_{\bar{\Omega}_h} + O(h^3)) + 4C^2O(h^2). \end{aligned} \quad (5.66)$$

According to the Lemma 2.3.2, we have

$$\|F_k\|_{\bar{\Omega}_h} = O(h^2), \|F^{reg}\|_{\bar{\Omega}_h} = O(h^2), \quad (5.67)$$

$$\|v\|_{\bar{\Omega}_h} \leq (5C^2 + 2C)O(h^2) + 2O(h^3). \quad (5.68)$$

This implies that:

$$\|p^h(\mathbf{j}h) - p^e(\mathbf{j}h)\|_{\bar{\Omega}_h} = O(h^2) \quad \text{for } \mathbf{j}h \in \Omega_h. \quad (5.69)$$

□

In next section, we prove the results of velocities in Theorem 5.2.1.

5.4 The accuracy of velocity

In this section, we show that velocity can reach second order accuracy when the pressure reaches second order accuracy. Consider the two velocity Poisson equations

$$\Delta u = p_x - (F_1 + g_1), \quad (5.70)$$

$$\left[\frac{\partial u}{\partial n} \right] = \hat{f}_2 \sin \theta, \quad (5.71)$$

$$\Delta v = p_y - (F_2 + g_2), \quad (5.72)$$

$$\left[\frac{\partial v}{\partial n} \right] = \hat{f}_2 \cos \theta, \quad (5.73)$$

$$[u] = 0, [v] = 0. \quad (5.74)$$

where θ is the angle between normal direction of the interface and horizontal axis, $\mathbf{g} = (g_1, g_2)^\top$ and $F = (F_1, F_2)^\top$.

We see that there are p_x and p_y on the right hand side of equations for u and v . We computed pressure from the previous Poisson equations for pressure numerically such that the error from the immersed interface method for pressure affect the solutions to velocities.

In the following subsection, we estimate $D_1^+(p^h - p^e)$ and $D_2^+(p^h - p^e)$.

5.4.1 The estimations of $D_1^+(p^h - p^e)$ and $D_2^+(p^h - p^e)$

Let $v = p^h - p^e$. We have already estimated $\|\nabla_h^+ v\|_{\overline{\Omega}_h}^2$ in Lemma 5.2.2. And we know $\nabla_h^+ v = (D_1^+ v, D_2^+ v)$ such that

$$\|D_1^+ v\| \leq \|\nabla_h^+ v\|, \quad (5.75)$$

$$\|D_2^+ v\| \leq \|\nabla_h^+ v\|. \quad (5.76)$$

In Lemma 5.2.2, we have

$$\begin{aligned} \|\nabla_h^+ v\|_{\overline{\Omega}_h}^2 &\leq \|F^{reg}\|_{\overline{\Omega}_h} \|v\|_{\overline{\Omega}_h} + (\|F_1\|_{\overline{\Omega}_h} + O(h^3)) \|D_1^+ v\|_{\overline{\Omega}_h} \\ &\quad + (\|F_2\|_{\overline{\Omega}_h} + O(h^3)) \|D_2^+ v\|_{\overline{\Omega}_h} + 4O(h^2) \|v\|_{\overline{\Omega}_h}. \end{aligned} \quad (5.77)$$

Combining with the inequalities $\|D_1^+ v\|_{\overline{\Omega}_h}^2 \leq \|\nabla_h^+ v\|_{\overline{\Omega}_h}^2$, $\|D_2^+ v\|_{\overline{\Omega}_h}^2 \leq \|\nabla_h^+ v\|_{\overline{\Omega}_h}^2$ and $\|v\|_{\overline{\Omega}_h} \leq C \|\nabla_h^+ v\|_{\overline{\Omega}_h}$,

$$\begin{aligned} \|D_1^+ v\|^2 &\leq \|\nabla_h^+ v\|_{\overline{\Omega}_h}^2 \leq \|F^{reg}\|_{\overline{\Omega}_h} \|v\|_{\overline{\Omega}_h} + (\|F_1\|_{\overline{\Omega}_h} + O(h^3)) \|D_1^+ v\|_{\overline{\Omega}_h} \\ &\quad + (\|F_2\|_{\overline{\Omega}_h} + O(h^3)) \|D_2^+ v\|_{\overline{\Omega}_h} + 4O(h^2) \|v\|_{\overline{\Omega}_h} \\ &\leq \|F^{reg}\|_{\overline{\Omega}_h} \|\nabla_h^+ v\|_{\overline{\Omega}_h} + (\|F_1\|_{\overline{\Omega}_h} + O(h^3)) \|D_1^+ v\|_{\overline{\Omega}_h} \\ &\quad + (\|F_2\|_{\overline{\Omega}_h} + O(h^3)) \|D_2^+ v\|_{\overline{\Omega}_h} + 4O(h^2) \|\nabla_h^+ v\|_{\overline{\Omega}_h}, \end{aligned} \quad (5.78)$$

$$\|D_2^+ v\|^2 \leq \|\nabla_h^+ v\|_{\overline{\Omega}_h}^2 \leq \|F^{reg}\|_{\overline{\Omega}_h} \|v\|_{\overline{\Omega}_h} + (\|F_1\|_{\overline{\Omega}_h} + O(h^3)) \|D_1^+ v\|_{\overline{\Omega}_h}$$

$$\begin{aligned}
& + (\|F_2\|_{\bar{\Omega}_h} + O(h^3))\|D_2^+v\|_{\bar{\Omega}_h} + 4O(h^2)\|v\|_{\bar{\Omega}_h} \quad (5.79) \\
& \leq \|F^{reg}\|_{\bar{\Omega}_h}\|\nabla_h^+v\|_{\bar{\Omega}_h} + (\|F_1\|_{\bar{\Omega}_h} + O(h^3))\|D_1^+v\|_{\bar{\Omega}_h} \\
& + (\|F_2\|_{\bar{\Omega}_h} + O(h^3))\|D_2^+v\|_{\bar{\Omega}_h} + 4O(h^2)\|\nabla_h^+v\|_{\bar{\Omega}_h}.
\end{aligned}$$

In the inequalities above, we divide the first inequality by $\|D_1^+v\|$ and the second by $\|D_2^+v\|$.

$$\begin{aligned}
\|D_1^+v\|_{\bar{\Omega}_h} & \leq \|F^{reg}\|_{\bar{\Omega}_h} \frac{\|\nabla_h^+v\|_{\bar{\Omega}_h}}{\|D_1^+v\|_{\bar{\Omega}_h}} + (\|F_1\|_{\bar{\Omega}_h} + O(h^3)) \\
& + (\|F_2\|_{\bar{\Omega}_h} + O(h^3)) \frac{\|D_2^+v\|_{\bar{\Omega}_h}}{\|D_1^+v\|_{\bar{\Omega}_h}} + 4O(h^2) \frac{\|\nabla_h^+v\|_{\bar{\Omega}_h}}{\|D_1^+v\|_{\bar{\Omega}_h}}, \quad (5.80) \\
\|D_2^+v\|_{\bar{\Omega}_h} & \leq \|F^{reg}\|_{\bar{\Omega}_h} \frac{\|\nabla_h^+v\|_{\bar{\Omega}_h}}{\|D_2^+v\|_{\bar{\Omega}_h}} + (\|F_1\|_{\bar{\Omega}_h} + O(h^3)) \frac{\|D_1^+v\|_{\bar{\Omega}_h}}{\|D_2^+v\|_{\bar{\Omega}_h}} \\
& + (\|F_2\|_{\bar{\Omega}_h} + O(h^3)) + 4O(h^2) \frac{\|\nabla_h^+v\|_{\bar{\Omega}_h}}{\|D_2^+v\|_{\bar{\Omega}_h}}.
\end{aligned}$$

When we do this division, we have to make sure that the dividend is nonzero. So assume that $\|D_1^+v\|_{\bar{\Omega}_h} \neq 0$ and $\|D_2^+v\|_{\bar{\Omega}_h} \neq 0$. With $\|D_1^+v\|_{\bar{\Omega}_h}$, $\|D_2^+v\|_{\bar{\Omega}_h}$ and $\|\nabla_h^+v\|_{\bar{\Omega}_h}$ finite, there exists K_1 , K_2 , K_3 , and K_4 large enough such that

$$\frac{\|\nabla_h^+v\|_{\bar{\Omega}_h}}{\|D_1^+v\|_{\bar{\Omega}_h}} \leq K_1, \quad \frac{\|D_2^+v\|_{\bar{\Omega}_h}}{\|D_1^+v\|_{\bar{\Omega}_h}} \leq K_2, \quad (5.81)$$

$$\frac{\|\nabla_h^+v\|_{\bar{\Omega}_h}}{\|D_2^+v\|_{\bar{\Omega}_h}} \leq K_3, \quad \frac{\|D_1^+v\|_{\bar{\Omega}_h}}{\|D_2^+v\|_{\bar{\Omega}_h}} \leq K_4. \quad (5.82)$$

With $\|F^{reg}\|_{\bar{\Omega}_h} = O(h^2)$, $\|F_1\|_{\bar{\Omega}_h} = O(h^2)$ and $\|F_2\|_{\bar{\Omega}_h} = O(h^2)$, we can have that

$$\|D_1^+v\|_{\bar{\Omega}_h} = O(h^2), \quad (5.83)$$

$$\|D_2^+ v\|_{\bar{\Omega}_h} = O(h^2), \quad (5.84)$$

which implies

$$\|D_1^+(p^h - p^e)\|_{\bar{\Omega}_h} = O(h^2), \quad (5.85)$$

$$\|D_2^+(p^h - p^e)\|_{\bar{\Omega}_h} = O(h^2). \quad (5.86)$$

With this result, in next subsection we will talk about the accuracy of velocity.

5.4.2 The accuracy of velocity u and v

In this subsection, we derive the accuracy of velocity. We first consider the situation when $\|D_1^+(p^h - p^e)\|_{\bar{\Omega}_h} \neq 0$ and $\|D_2^+(p^h - p^e)\|_{\bar{\Omega}_h} \neq 0$. In the previous subsection, we have already had

$$\|D_1^+(p^h - p^e)\|_{\bar{\Omega}_h} = O(h^2), \quad (5.87)$$

$$\|D_2^+(p^h - p^e)\|_{\bar{\Omega}_h} = O(h^2), \quad (5.88)$$

Thus, combining with the Poisson equations for velocities u and v ³, we have

$$\Delta_h(u^h - u^e) = O(h^2), \quad u^h - u^e = 0 \quad \text{on} \quad \partial\Omega_h, \quad (5.89)$$

$$\Delta_h(v^h - v^e) = O(h^2), \quad v^h - v^e = 0 \quad \text{on} \quad \partial\Omega_h, \quad (5.90)$$

³In this subsection, v represents velocity in vertical direction.

with jump conditions. From the result in [2], we can have that

$$|u^h - u^e| = O(h^2), \quad (5.91)$$

$$|v^h - v^e| = O(h^2), \quad (5.92)$$

on the computation domain Ω_h . This means that the numerical solution of velocities reach second order accuracy.

Next, we consider the situation when $\|D_1^+(p^h - p^e)\|_{\bar{\Omega}_h} = 0$ but $\|D_2^+(p^h - p^e)\|_{\bar{\Omega}_h} \neq 0$. It implies that $\|D_1^+(p^h - p^e)\|_{\bar{\Omega}_h} = 0$ such that $D_1^+p^h = D_1^+p^e$. In this situation,

$$\Delta_h(u^h - u^e) = O(h^2), \quad u^h - u^e = 0 \quad \text{on} \quad \partial\Omega_h. \quad (5.93)$$

From the result in [2], $|u^h - u^e| = O(h^2)$ in Ω_h .

On the other side for $\|D_2^+(p^h - p^e)\|_{\bar{\Omega}_h}$, $\|\nabla_h^+(p^h - p^e)\|_{\bar{\Omega}_h} = \|D_2^+(p^h - p^e)\|_{\bar{\Omega}_h}$. Back to the inequality of $\|D_2^+(p^h - p^e)\|_{\bar{\Omega}_h}$,

$$\begin{aligned} \|D_2^+(p^h - p^e)\|_{\bar{\Omega}_h} &\leq \|F^{reg}\|_{\bar{\Omega}_h} + (\|F_1\|_{\bar{\Omega}_h} + O(h^3)) \frac{\|D_1^+(p^h - p^e)\|_{\bar{\Omega}_h}}{\|D_2^+(p^h - p^e)\|_{\bar{\Omega}_h}} \\ &\quad + (\|F_2\|_{\bar{\Omega}_h} + O(h^3)) + 4O(h^2). \end{aligned} \quad (5.94)$$

From the inequality of $\|\nabla_h^+(p^h - p^e)\|_{\bar{\Omega}_h}$, we know that $\|D_1^+(p^h - p^e)\|_{\bar{\Omega}_h}$ and $\|D_2^+(p^h - p^e)\|_{\bar{\Omega}_h}$ are finite such that

$$\frac{\|D_1^+(p^h - p^e)\|_{\bar{\Omega}_h}}{\|D_2^+(p^h - p^e)\|_{\bar{\Omega}_h}} = 0. \quad (5.95)$$

With $\|F^{reg}\|_{\overline{\Omega}_h} = O(h^2)$, $\|F_1\|_{\overline{\Omega}_h} = O(h^2)$ and $\|F_2\|_{\overline{\Omega}_h} = O(h^2)$, we have

$$\|D_2^+(p^h - p^e)\|_{\overline{\Omega}_h} = O(h^2), \quad (5.96)$$

such that

$$\Delta_h(v^h - v^e) = O(h^2), \quad v^h - v^e = 0 \quad \text{on} \quad \partial\Omega_h, \quad (5.97)$$

with jump conditions. From the result in [2], we have

$$|v^h - v^e| = O(h^2). \quad (5.98)$$

We can show the same result in similar way for situations when $\|D_2^+(p^h - p^e)\|_{\overline{\Omega}_h} = 0$ but $\|D_1^+(p^h - p^e)\|_{\overline{\Omega}_h} \neq 0$ and when both of them are zeros. It implies that both of the velocities on horizontal and vertical direction can reach second order accuracy no matter whether $\|D_1^+(p^h - p^e)\|_{\overline{\Omega}_h}$ and $\|D_2^+(p^h - p^e)\|_{\overline{\Omega}_h}$ are zeros.

5.5 Conclusion

In this Chapter, we consider the Stokes equation with an interface. We have the result that the immersed interface method can give second order accurate solution with three Poisson equations approach, while most of numerical methods can only reach first order accuracy for pressure. Additionally, the numerical solution of velocity also reach second order accuracy with the immersed interface method even though the error generated from numerical solution of pressure would affect the problems of velocity.

Chapter 6

CONCLUSION AND FUTURE WORK

6.1 Summary

Our work in error analysis of the immersed interface method is completing the theoretical proof which is missing for the interface problem with a Neumann boundary condition.

We point out the main contributions of our work:

- We showed that the immersed interface method gives second-order accurate solution for Poisson equation with an interface, constant coefficients and Neumann boundary conditions.
- We extend the results from the maximum principle and Theorem (6.1) and (6.2) in [16] for the problems with a Neumann boundary condition.
- We showed that the numerical solution from the immersed interface method reaches second-order accuracy for the Poisson equation with an interface, a variable

coefficient $\beta(x)$ and Neumann boundary conditions.

- We showed that for a complicated elliptic problem $(\beta u_x)_x - \sigma^2 u = f$ with an interface and Neumann boundary conditions, the immersed interface method also gives second-order accurate numerical solution.
- We proved that the immersed interface method with three-Poisson-equations approach has second-order accurate solution for both pressure and velocity in the Stokes equations with an interface.

6.2 Future work

During our work, we have talked about the Poisson equations, the equation $(\beta u_x)_x - \sigma^2 u = f$ and the Stokes equations. However, these are only a little piece of elliptic problems. We focused on our attention on the problems with Neumann boundary conditions. But for those interface problems which have mixed boundary conditions, we don't know whether the immersed interface method can still give second-order accurate solution.

When we talked about the elliptic problem $(\beta u_x)_x - \sigma^2 u = f$, we assume that $2\beta - \sigma^2 > 0$. This assumption makes this problem more specific. Actually, from the finite difference scheme, the problem has unique solution for any coefficient σ . The results from the maximum principle and related theorems should work on a more general problem. So finding a better comparison function for this problem should be one part of the future work such that it can help to extend the error analysis to a general problem regardless of the value of σ . We have worked on the one-dimensional elliptic problem for this. The error analysis of higher dimensional problems should be contained in the future work.

We have shown that the immersed interface method is efficient for the Stokes prob-

lem with an interface. However, the Navier-Stokes equations are the famous system in computational fluid dynamics. The error analysis of the immersed interface method for the Navier-Stokes equations is still missing. There is a lot of work can be done in this part.

We notice that we used two different approaches to prove our result based on the types of problems. And the approaches work for some specific problems. For other elliptic problems, they may not work. Comparing the two approaches, they have their own advantages and disadvantages. The biggest difference between these two approaches is finding comparison functions. If we can find a comparison function for each elliptic problem, we can show error analysis of every elliptic problem. The approach by using results from the maximum principle and related theorems seems to be more general. But finding comparison functions is the most difficult part during error analysis. The way to construct a good comparison function should be one important part in our future research.

BIBLIOGRAPHY

- [1] L.M. Adams. A multigrid algorithm for immersed interface problems. *NASA Conference Publication 3339*, (1-14), 1995.
- [2] J. Thomas Beale and Anita T. Layton. On the accuracy of finite difference methods for elliptic problems with interfaces. 2006.
- [3] M.J. Berger and R.J.LeVeque. Adaptive mesh refinement using wavepropagation algorithms for hyperbolic systems. *SIAM J. Numer. Anal.*, 35(2298-2316), 1998.
- [4] C.S.Peskin. Numerical analysis of blood flow in the heart. *Journal of Computational Physics*, 25(220-252), 1977.
- [5] C.S.Peskin. Lectures on mathematical aspects of physiology. *Lectures in Appl. Math.*, 19(69-107), 1981.
- [6] C.S.Peskin and D.M.McQueen. A three-dimensional computational method for blood flow in the hear:(i) immersed elastic fibers in a viscous incompressible fluid. *Journal of Computational Physics*, 81(372-405), 1989.
- [7] C.S.Peskin and D.M.McQueen. A three-dimensional computational method for blood flow in the hear:(ii) contractile fibers. *Journal of Computational Physics*, 82(289-297), 1989.
- [8] C.S.Peskin and D.M. McQueen. A general method for the computer simulation of biological systems interacting with fluids. *Symposia of the Society for Experimental Biology*, 49(265), 1995.
- [9] Huaxiong Huang and Zhilin Li. Convergence analysis of the immersed interface method. *IMA Journal of Numerical Analysis*, 19(583-608), 1999.
- [10] P. Swarztrauber J. Adams and R. Sweet. Fishpack: Efficient fortran subprograms for the solution of separable elliptic partial differential equations. <http://www.netlib.org/fishpack/>.
- [11] J.A.Sethian. Level set methods and fast marching methods. *Cambridge University Press*, 1999.
- [12] C.N. Dawson J.B. Bell and G.R. Shubin. An unsplit, higher order godunov method for scalar conservation laws in multiple dimensions. *J.Comput.Phys.*, 74(1-24), 1988.
- [13] Hans Johnston and Jian-Guo Liu. Finite difference schemes for incompressible flow based on local pressure boundary conditions. *Journal of Computational Physics*, 180(120-154), 2002.

- [14] Hans Johnston and Jian-Guo Liu. Accurate, stable and efficient navier-stokes solvers based on explicit treatment of the pressure term. *Journal of Computational Physics*, 199(221-259), 2004.
- [15] J. Kevorkian. Partial differential equations. Wadsworth and Brook/Cole Mathematics Series, 1990.
- [16] K.W.Morton and David Mayers. *Numerical Solution of Partial Differential Equations Second Edition*. Cambridge University Press, 2005.
- [17] Randall J. Leveque and Zhilin Li. The immersed interface method for elliptic equations with discontinuous coefficients and singular sources. *SIAM J. NUMER. ANAL.*
- [18] Randall J. Leveque and Zhilin Li. Immersed interface methods for stokes flow with elastic boundaries or surface tension.
- [19] Z. Li. An overview of the immersed interface method and its applications. *J. Math.*, 7(1-49), 2003.
- [20] Z. Li. An augmented cartesian grid method for stokes-darcy fluid-structure interactions. *International Journal of Computer Mathematics*, 106(556-575), 2015.
- [21] Z. Li and K. Ito. Maximum principle preserving schemes for interface problems with discontinuous coefficients. *SIAM J. Sci. Comput*, 23(339-361), 2001.
- [22] Z. Li and K. Ito. The immersed interface method-numerical solutions of pdes involving interfaces and irregular domains. *SIAM Frontier Series in Applied Mathematics*, FR33, 2006.
- [23] C. S. Peskin. The immersed boundary method. *Acta Numerica*, (1-39), 2002.
- [24] R.J.LeVeque. Clawpack and amrclaw-software for high-resolution godunov methods. *4-th Intl. Conf. on Wave Propagation*, 1998.
- [25] V. Rutka. A fast numerical method for the computation of effective elastic moduli of 3d fibrous microstructures. *University of Kaiserslautern*, MS. Thesis, 2001.
- [26] G.R. Shubin and J.B. Bell. An analysis of the grid orientation effect in numerical simulation of miscible displacement. *Comp. Meth. Appl. Mech. Eng.*, 47(47-71), 1984.
- [27] S.Osher and J.A.Sethian. Fronts propagating with curvature-dependent speed: Algorithms based on hamilton-jacobi formulations. *Journal of Computational Physics*, 79(12-49), 1988.

- [28] S.Osher and R.Fedkiw. Level set methods and dynamic implicit surfaces. *Springer*, 2002.
- [29] Paul N. Swarztrauber. Fast poisson solver. *Studies in Numerical Analysis*, 24(319-370), 1984.
- [30] A.N. Tikhonov and A.A. Samarskii. Homogeneous difference schemes. *USSR Comput. Math. and Math. Phys.*, 1(5-67), 1962.
- [31] A.-K. Tornberg. Regularization techniques for singular source terms in differential equations. *ECM Stockholm, European Mathematical Society*, (477-499), 2005.
- [32] A.-K. Tornberg and B. Engquist. Regularization techniques for numerical approximation of pdes with singularities. *Journal of Scientific Computing*, 19(527-552), 2003.
- [33] M. Lai Z. Li, K. Ito. An augmented approach for stokes equations with discontinuous viscosity and singular forces. *Computers and Fluids*, 36(622-635), 2007.
- [34] D.De Zeeuw. Matrix-dependent prolongations and restrictions in a blackbox multi-grid solver. *J.Comput.Appl.Math.*, 33(1-27), 1990.